SUBMITTED TO THE ASTROPHYSICAL JOURNAL: SEPTEMBER 6 2011
Preprint typeset using LaTeX style emulateapj v. 11/10/09

arXiv:1110.3786v1 [astro-ph.CO] 17 Oct 2011

WHAT TURNS GALAXIES OFF? THE DIFFERENT MORPHOLOGIES OF STAR-FORMING AND QUIESCENT GALAXIES SINCE $Z \sim 2$ FROM CANDELS

ERIC F. BELL[1], ARJEN VAN DER WEL[2], CASEY PAPOVICH[3], DALE KOCEVSKI[4], JENNIFER LOTZ[5], DANIEL H. MCINTOSH[6], JEYHAN KARTALTEPE[7], S. M. FABER[4], HARRY FERGUSON[5], ANTON KOEKEMOER[5], NORMAN GROGIN[5], STIJN WUYTS[8], EDMOND CHEUNG[4], CHRISTOPHER J. CONSELICE[9], JAMES S. DUNLOP[10], MAURO GIAVALISCO[11], JESSICA HERRINGTON[1], DAVID KOO[4], ELIZABETH J. MCGRATH[4], DUILIA DE MELLO[12,13], HANS-WALTER RIX[2], ADAY R. ROBAINA[14], CHRISTINA C. WILLIAMS[11]

[1] Department of Astronomy, University of Michigan, 500 Church St., Ann Arbor, MI 48109, USA; ericbell@umich.edu
[2] Max-Planck Institut für Astronomie, Königstuhl 17, D-69117, Heidelberg, Germany
[3] George P. and Cynthia Woods Mitchell Institute for Fundamental Physics and Astronomy, and Department of Physics and Astronomy, Texas A&M University, College Station, TX 77843-4242, USA
[4] University of California Observatories/Lick Observatory, University of California, Santa Cruz, CA 95064, USA
[5] Space Telescope Science Institute, 3700 San Martin Drive, Baltimore, MD 21218, USA
[6] Department of Physics, University of Missouri-Kansas City, Kansas City, MO 64110, USA
[7] NOAO-Tucson, 950 North Cherry Ave., Tucson, AZ 85719
[8] Max-Planck-Institut für Extraterrestrische Physik, Giessenbachstrasse, D-85748 Garching, Germany
[9] University of Nottingham, School of Physics and Astronomy, Nottingham NG7 2RD, UK
[10] Institute for Astronomy, University of Edinburgh, Royal Observatory, Blackford Hill, Edinburgh EH9 3HJ, UK
[11] Department of Astronomy, University of Massachusetts, Amherst, MA 01003, USA
[12] Department of Physics, The Catholic University of America, Washington, D.C. 20064
[13] Observational Cosmology Laboratory, Goddard Space Flight Center, Code 665, Greenbelt, MD 20771
[14] Institut de Ciencies del Cosmos, ICC-UB, IEEC, Marti i Franques 1, 08028, Barcelona, Spain

SUBMITTED TO THE ASTROPHYSICAL JOURNAL: *September 6 2011*

ABSTRACT

We use HST/WFC3 imaging from the CANDELS multicycle treasury survey, in conjunction with the Sloan Digital Sky Survey, to explore the evolution of galactic structure for galaxies with stellar masses $> 3 \times 10^{10} M_{\odot}$ from $z = 2.2$ to the present epoch, a time span of 10 Gyr. We explore the relationship between rest-frame optical color, stellar mass, star formation activity and the structural parameters of galaxies as determined from parametric fits to the surface brightness profiles of galaxies. We confirm the dramatic evolution from $z = 2.2$ to the present day in the number density of non-star-forming galaxies above $3 \times 10^{10} M_{\odot}$ reported by other authors. We find that the vast majority of these quiescent systems have concentrated light profiles, as parameterized by the Sérsic index, and the population of concentrated galaxies grows similarly rapidly. We examine the joint distribution of star formation activity, Sérsic index, stellar mass, mass divided by radius (a proxy for velocity dispersion), and stellar surface density. Quiescence correlates poorly with stellar mass at all $z < 2.2$ (given the $\lesssim 0.2$ dex scatter between halo mass and stellar mass at $z \sim 0$ inferred by More et al. 2009; MNRAS, 392, 801, this argues against halo mass being the only factor determining quiescence). Quiescence correlates better with Sérsic index, 'velocity dispersion' and stellar surface density, where Sérsic index correlates the best (increasingly so at lower redshift). Yet, there is significant scatter between quiescence and galaxy structure: while the vast majority of quiescent galaxies have prominent bulges, many of them have significant disks, and a number of bulge-dominated galaxies have significant star formation. Noting the rarity of quiescent galaxies without prominent bulges, we argue that a prominent bulge (and, perhaps by association, a supermassive black hole) is a necessary but not sufficient condition for quenching star formation on galactic scales over the last 10 Gyr; such a result is qualitatively consistent with the expectations of the AGN feedback paradigm.

Subject headings: galaxies: elliptical and lenticular, cD — galaxies: structure — galaxies: evolution — galaxies: general

1. INTRODUCTION

The last decade of study has brought into sharper focus than ever the bimodality of the star formation histories of galaxies. There is a relatively tight distribution of star formation rates (SFRs) at a given mass for star forming galaxies (~ 0.3 dex scatter, with a few outliers to high SFR; e.g., Brinchmann et al. 2004, Salim et al. 2007), persisting out to $z > 2$ (Noeske et al. 2007; Wuyts et al. 2011a). The red sequence has SFRs substantially below those expected for star forming galaxies (but often with some star formation; see, e.g., Yi et al. 2005). We will call these quiescent galaxies in what follows. The relative prominence of the two populations is a function of stellar mass, surface density, inferred velocity dispersion $M/R \propto \sigma^2$, and galaxy structure (e.g., Strateva et al. 2001; Kauffmann et al. 2003; Blanton et al. 2003; Franx et al. 2008; Bell 2008). This correlation between the structural properties of galaxies with their stellar populations is important: it signals that the processes that determine the structures of galaxies at least correlate, and perhaps are the same as, the processes that shape whether or not a galaxy has cold gas and star formation. Furthermore, these two populations evolve in their relative importance: while the star-forming population has a stellar mass function that evolves slowly (Borch et al. 2006; Bell et al. 2007; Peng et al. 2010; Brammer et al. 2011), the quiescent galaxy stellar mass function evolves rapidly from $z \sim 2$ to the present day (largely in normalization by factors of ~ 10,

but with modest or no evolution in shape or 'characteristic' mass M^*; Bell et al. 2004; Borch et al. 2006; Faber et al. 2007; Brown et al. 2007; Taylor et al. 2009; Peng et al. 2010; Domínguez Sánchez et al. 2011; Brammer et al. 2011).

A great deal of work, both theoretical and observational, has been carried out to try to better understand the drivers of the evolution of these two populations, particularly why some galaxies appear capable of shutting off their star formation while others are incapable of doing so. In this study, we will focus on processes that can shut down star formation in galaxies which reside in the center of their own dark matter halo. The clear effects of gas removal/starvation in dense environments (see, e.g., van der Wel et al. 2010, Peng et al. 2010, Weinmann et al. 2010, Peng et al. 2011, Weinmann et al. 2011 for recent discussions of this issue using survey datasets) are only a minor contributor to the evolution of 'cosmic averaged' galaxy population, owing to the small number of galaxies inhabiting dense environments (Peng et al. 2010). Accordingly, we do not discuss the effect of environment in this paper (see, e.g., Peng et al. 2010 for a careful discussion of the effects of environment as a function of cosmic time). An important point is that models that include the growth of the dark matter framework, gas cooling, star formation and stellar feedback alone fail to predict a widespread population of non-star-forming galaxies (Benson et al. 2003; Cattaneo et al. 2006; Somerville et al. 2008; Davé et al. 2011); all galaxies are expected to accrete (or cool) cold gas and form stars.

A number of possible mechanisms have been proposed to keep a galaxy in the center of its own halo free of a significant cold gas content. Noting the strong tendency of quiescent galaxies to have prominent (or dominant) bulge components, it has long been thought that merging plays an important role in determining their structure (e.g., Toomre & Toomre 1972; Barnes & Hernquist 1992; Hernquist 1993; Naab et al. 2006; Hoffman et al. 2010). The approximate equality of the merger rate and the quiescent galaxy formation rate (e.g., Hopkins et al. 2010; Robaina et al. 2010), the detailed kinematic structure of early-type galaxies (Naab et al. 2006; Hoffman et al. 2010), and the empirical association between relatively younger stellar populations and substructure (tidal tails, shells, asymmetries, etc.) in quiescent galaxies (Schweizer & Seitzer 1992; Tal et al. 2009; Győry & Bell 2010) are qualitatively (and to a certain extent quantitatively) consistent with this picture.

Largely in this merger context, the possibility that feedback from accretion onto a supermassive black hole may drive gas out of galaxies (Kauffmann & Haehnelt 2000; Springel et al. 2005) or keep gas around galaxies from cooling (Croton et al. 2006; Somerville et al. 2008) has been explored enthusiastically. A wide array of observations are, at least at face value, qualitatively consistent with such a picture: e.g., galaxies with big bulges have big black holes (Magorrian et al. 1998; Gültekin et al. 2009), low-redshift galaxies without prominent bulges cannot shut off their star formation on their own (Bell 2008), rapid large-scale winds are observed around post-starburst galaxies and quasars (Tremonti et al. 2007; Prochaska & Hennawi 2009), and the energy measured in AGN-inflated outflow cavities in the hot gas atmosphere of groups and clusters of galaxies is approximately consistent with the energy required to offset cooling (Best et al. 2006; Fabian et al. 2006). There are a number of other possible mechanisms for shutting off star formation, however. A few examples are: the heating of the gaseous halo through virialization of the gas content (Naab et al. 2007; Dekel & Birnboim 2008; Khochfar & Ostriker 2007; Johansson et al. 2009), changes in the mode of gas accretion onto galaxies as a function of dark matter halo mass (Kereš et al. 2005; Dekel & Birnboim 2006; Cattaneo et al. 2006; Birnboim et al. 2007), and the heating of large halos with energy from cosmic rays (Guo & Oh 2008).

1.1. *The goal of this paper*

Given the range of possible mechanisms for shutting off star formation on galactic scales for galaxies in the center of their own halos, gathering empirical insight into the properties of non star-forming galaxies, as a function of cosmic epoch, can be helpful. It has been argued that the key parameter that correlates with the paucity of star formation is stellar surface density (Kauffmann et al. 2003; Franx et al. 2008), or possibly velocity dispersion (or roughly equivalently as M/R; Franx et al. 2008). Yet, for a sample of low-redshift galaxies from the SDSS, Bell (2008) instead argues that Sérsic index correlates much better with a lack of star formation for galaxies in the center of their own halo (that could not have been stripped of their gas by external influences), as non-star forming galaxies have high Sérsic indices but a range of surface densities that overlap with star-forming galaxies. Such an investigation has not been carried out at $z \gtrsim 1$, owing to a lack of large-scale near-IR HST imaging until recently (see, e.g., Kriek et al. 2009, Cameron et al. 2010, and Szomoru et al. 2011 for early progress towards this goal at $z \sim 2$; Wuyts et al. 2011b explores this in more depth).

A not inconsiderable challenge in achieving this goal is the definition of what constitutes star-forming or quiescent galaxies. At a given stellar mass, the SFR of galaxies depends strongly on redshift, evolving by a factor of 5–10 by $z \sim 1$ and another factor of 4 or so out to $z \sim 2$ (Zheng et al. 2007; Noeske et al. 2007; Dunne et al. 2009; Karim et al. 2011). Noting that the scatter in SFR at a given stellar mass is modest (a factor of $\lesssim 2$; Noeske et al. 2007), one could choose to define a quiescent galaxy as one that has a SFR more than 1σ below the star forming galaxy locus at the redshift of interest, and a star-forming galaxy as any galaxy forming stars at a higher rate. An alternative approach is to separate galaxies by their optical–near-IR colors (e.g., $U-V/V-J$; Wuyts et al. 2007, Williams et al. 2009), where galaxies dominated by old stellar populations are distinguishable from star-forming galaxies with even substantial dust reddening (as used by e.g., Williams et al. 2009 and Brammer et al. 2011). In this paper, we adopt both techniques. We note that a galaxy at $z \sim 2$ which is defined as quiescent according to these two criteria may have a SFR considerably in excess of almost all star-forming disk galaxies at the present day. While this means that our sample of quiescent galaxies does not have identical properties across all redshifts, it does isolate a sample of galaxies with unusually low SFRs at that epoch given their stellar masses (confirmed by 24μm stacking) — one would like to understand why their SFRs are unusually low at that epoch.

In this paper, we explore the evolution of the structures of galaxies as a function of redshift, and how they relate to the star formation activity in those galaxies. We use new near-infrared imaging from the Wide Field Camera 3 (WFC3) on the *Hubble Space Telescope* taken as part of the Cosmic Assembly Near-IR Deep Extragalactic Legacy Survey (CANDELS) multi-cycle treasury program (Grogin et al. 2011; Koekemoer et al. 2011), focusing on the $0.6 < z <$

2.2 galaxy population in the UKIRT IR Deep Sky Survey (UKIDDS; Lawrence et al. 2007) Ultradeep Survey (UDS; §2). These data allow us to explore the structure of the $M_* > 3 \times 10^{10} M_\odot$ galaxy population in the rest-frame optical to $z \lesssim 2.2$. We supplement this with data from the Sloan Digital Sky Survey Data Release 2 (Abazajian et al. 2004) to connect with the properties of local galaxies. We perform two basic analyses to explore the evolution of the galaxy population. First, we explore the evolution of the galaxy population drawn from an 'equivalent' constant comoving volume as a function of redshift, to get a sense of how the star formation and structural properties of the galaxy population evolves with cosmic epoch (§3). Second, we explore the relationship between the structural parameters of galaxies and their star formation activity using the full sample at each epoch to maximize number statistics, in an attempt to understand which structural parameters best correlate with a lack of star formation activity (§4).In what follows, we use Vega magnitudes for rest-frame colors, assume that every star ever formed does so according to a universally-applicable Chabrier (2003) stellar IMF, and assume $H_0 = 70\,\mathrm{km\,s^{-1}\,Mpc^{-1}}$, $\Omega_{m,0} = 0.3$ and $\Omega_{\Lambda,0} = 0.7$.

2. DATA

2.1. *UDS imaging data*

Our sample definition and selection is based on the public K-band selected photometric catalog produced by Williams et al. (2009)[1]. We adopt these redshifts in this paper as the basis for conversion of apparent magnitudes into rest-frame colors, magnitudes and stellar masses, and the conversion of apparent to physical sizes. The Williams et al. (2009) catalog uses J and K-band data for the UKIDDS UDS Data Release 1 (Lawrence et al. 2007; Warren et al. 2007) in conjunction with B, R, i and z-band imaging from the SXDS (Furusawa et al. 2008) and 3.6μm and 4.5μm IRAC imaging data taken as part of the SWIRE survey (Lonsdale et al. 2003). Total fluxes were calculated using an elliptical Kron (1980) aperture, and observed-frame fluxes were calculated using a matched 1.″75 circular aperture on PSF-matched images (with the obvious exception of the poorer resolution IRAC imaging data, whose fluxes were measured in 3″ apertures and aperture corrected to the smaller aperture size). Finally, Williams et al. (2009) used the EAZY photometric redshift code (Brammer et al. 2008) to estimate photometric redshift from the photometric catalogs.

Spectroscopic redshifts for the UDS are relatively few in number and preferentially focus on brighter sources; for these sources with $z_{\rm spec} \lesssim 1.1$ the redshift normalized median absolute deviation (the median absolute deviation, renormalized to give the same value as the RMS of a Gaussian distribution) of $|z_{\rm phot} - z_{\rm spec}|/(1+z_{\rm spec})$ is ~ 0.033 with 8% catastrophic outliers (Williams et al. 2009). We have also compared the Williams et al. (2009) photometric redshifts against those of S. Wuyts et al. (in prep.), who used completely different (deeper) photometry and a similar photoz code to estimate photoz for galaxies in the CANDELS/UDS coverage, finding a $\Delta z/(1+z_{\rm Williams}) \sim 0.055$, and $\sim 10\%$ catastrophic outliers (defined as having $|\Delta z|/(1+z_{\rm Williams}) > 0.2$. We have confirmed that use of the photometric redshifts, k-corrections and stellar masses from Wuyts et al. instead of the public Williams et al. (2009) photometric redshifts plus the rest-frame colors and masses reported here yields no significant changes to our results.

To explore the structure and morphology of the $0.6 < z < 2.2$ galaxy population, we use near-infrared F160W imaging from the HST, using the WFC3. CANDELS is a HST multi-cycle treasury program (PIs: S. Faber & H. Ferguson, PID: GO-12060) to image five fields on the sky using the WFC3 and Advanced Camera for Surveys (ACS). The CANDELS imaging of the UDS field imaging includes 2/3 orbit in F125W and 4/3 orbits in F160W split into two epochs (see Koekemoer et al. 2011 and Grogin et al. 2011 for more details). A total of 44 WFC3 tiles were imaged in the UDS; when cross-matched with the Williams et al. (2009) catalog a total of 0.056 square degrees were covered.

We use also 24μm flux as a diagnostic to aid in the separation between galaxies with active star formation, and those with little or no star formation. We use 24μm public data from the SpUDS survey [2] of the UDS. PSF fitting photometry with a 13″ radius was performed, aperture corrected to total flux; the limiting flux of the catalog is $\sim 50\mu$Jy at the $\sim 80\%$ completeness (or 4σ level), and uncertainties in 24μm flux are of order $\sim 20\%$ (largely reflecting uncertainties in converting aperture to total flux, and source confusion).

2.2. *Rest-frame quantities and stellar masses*

The rest-frame magnitudes and stellar masses used in this paper were calculated using a set of template spectral energy distributions from the PEGASE stellar population models (see Fioc & Rocca-Volmerange 1997 for description of an earlier version of this stellar population model). Such stellar population models give very similar results to those of Bruzual & Charlot (2003), and stellar masses ~ 0.15 dex higher than the models by Maraston (2005)[3]. These stellar population templates have solar metallicity, and we allow for dust attenuation following Calzetti (2001), with values of gas $E(B-V)$ between -0.05 and 1.5 (to provide a little flexibility to fit negative attenuation to account for small photometry problems, etc.; in practice small negative attenuation values are rare in the fits presented here). The templates included a broad range of exponentially-decreasing, constant or exponentially rising star formation histories, beginning at $z_f \sim 4$ (see Maraston et al. 2010 for a discussion of the importance of exponentially rising star formation histories for fitting $z \gtrsim 2$ SEDs).

The templates treat the evolving galaxy population self-consistently, in the sense that all the galaxies that are in the $z = 2$ template set also appear in, e.g., the $z = 1$ or $z = 0.6$ template sets further along their evolutionary path. Thus, the galaxy population at lower redshifts is required to have substantial older stellar populations, driving up somewhat the typical age of the stars and the typical stellar mass-to-light ratio at a given color. This is to be contrasted with other codes (e.g., Wuyts et al. 2008 or Pannella et al. 2009) which have redshift-independent template sets, but exclude those tem-

[1] We choose to use this public catalog instead of other proprietary catalogs to better facilitate comparison with previous works and to allow easier reproduction of the results. We confirm that the results and conclusions do not significantly change if repeated with the redshifts, colors and stellar masses from the currently proprietary catalog of S. Wuyts et al. (in preparation).

[2] http://irsa.ipac.caltech.edu/data/SPITZER/SpUDS

[3] Although note that Kriek et al. (2010) demonstrate that the Bruzual & Charlot (2003) models appear to fit the optical–near-IR SEDs of galaxies with large intermediate-age stellar populations substantially better than Maraston (2005) models do. The overall mass scale offsets between Bruzual & Charlot (2003) and Maraston (2005) models have been discussed by a number of papers, and recently by e.g., Brammer et al. (2011) and Domínguez Sánchez et al. (2011).

plates that start star formation before the Big Bang — the typical stellar populations of galaxies with this type of template fit end up being significantly younger than in the method discussed here. It is unclear to us at this stage which method is more realistic; we will explore this issue with star formation histories drawn from a semi-analytic model of galaxy formation in a future paper (see, e.g., Lee et al. 2010 for a version of this exercise at higher redshift).

These templates were compared with photometric data points of each galaxy, given the photometric redshift value from Williams et al. (2009), and the template with the smallest χ^2 was used to calculate rest-frame colors and a stellar M/L ratio. Rest-frame magnitudes were calculated by using the SED shape of the template to work out the predicted rest-frame magnitude of the object given the two nearest observed-frame bands, and then performing a weighted average of those two estimates of rest-frame magnitude. Stellar masses were estimated using the stellar M/Ls of the best-fitting template, referenced to the three longest observed wavelengths for overall normalization. We note that the inclusion of dust, while it improves the quality of SED fit, leads to modest changes in the rest-frame colors and stellar masses of the sample explored in this paper, given the overall degeneracy between the effects of dust extinction and stellar population age in the optical–near–IR spectral region; Bell & de Jong 2001).

This method, when applied to galaxies with independently-estimated stellar masses (from independent photometry of similar but not identical datasets) in this field (S. Wuyts et al., in prep.) either the GOODS-S field (Wuyts et al. 2008) or COSMOS field (Pannella et al. 2009), yields similar masses for intensely star-forming galaxies, and masses ~ 0.2 dex larger for more dusty star-forming galaxies or non-star-forming galaxies (as the templates used here are more dominated by older stellar populations than the those used by Wuyts et al. 2008 or Pannella et al. 2009), with a scatter of 0.2 dex. Rest-frame colors are reproduced to within 0.1 mag. When this method is compared with the masses of Bell et al. (2003), calculated on identical photometry and using a more restricted set of stellar population models without dust, there is no offset and 0.07 dex scatter in stellar masses, and a scatter of less than 0.05 mag in rest-frame $U-V$ color.

We adopt the stellar mass estimates described above for the purposes of this paper to ensure consistency of the stellar mass estimation method and stellar mass scale as a function of redshift (the same code was used to estimate stellar masses at all redshifts, and the choice of templates evolves consistently from redshift to redshift). We have confirmed that the systematic discrepancies in stellar mass between the masses adopted here and those by, e.g., Wuyts et al. (2008) would operate to strengthen our conclusions (or in the case of the second part of the paper, leave them unaffected); their stellar masses for $z > 0.6$ galaxies are systematically lower by up to a factor of 2, with a factor of 2 scatter, and the evolution of the population would appear more rapid than it appears in this paper. In what follows we adopt a mass limit of $3 \times 10^{10} M_{\odot}$; the sample is 'complete' above this limit[4]. The masses and rest-frame magnitudes of the sample presented in this paper are available for download at: http://www.astro.lsa.umich.edu/~ericbell/data.php

[4] We say 'complete' because we filter the sample through steps that have uncertainties, e.g., photometric redshift or stellar mass estimation. We have confirmed that if we repeat the analysis with the Wuyts et al. sample, masses and rest-frame colors, drawn from deeper imaging data, our results and conclusions do not significantly change.

2.3. *Sérsic profile fits of* $0.6 < z < 2.2$ *galaxies*

To describe the structure of the galaxy population at $0.6 < z < 2.2$, we use parametric Sérsic (1968) fits to the galaxy images (A. van der Wel et al., in preparation). A surface brightness profile of the form $\Sigma(r) = \Sigma_e exp[-\kappa(\frac{r}{r_e}^{1/n} - 1)]$ is fit using the GALFIT package (Peng et al. 2002), and the GALAPAGOS wrapper[5], allowing the magnitude, axis ratio b/a, position angle, half-light radius r_e, Sérsic index n, and central position to be free parameters. The Sérsic index n describes the shape of the light profile, where $n = 1$ corresponds to an exponential light profile and $n = 4$ corresponds to a $r^{1/4}$ law profile characteristic of massive, spheroid-dominated early-type galaxies. The Sérsic parameter n is a reasonably good proxy for the ratio of bulge luminosity to total luminosity, as illustrated in Fig. 14 of Simard et al. (2011) — systems with high n invariably host a prominent bulge, whereas systems with low n host a weak or no bulge component. At the depths typical of this imaging, uncertainties in the fit parameters are $\delta \log_{10} n \sim 0.15$ dex, $\delta r_e \sim 18\%$, and $\delta b/a \sim 0.07$, as constrained from independent GALFIT analyses on F105W imaging of a subsample of $z \sim 1.6$ galaxies in the UDS (Papovich et al. 2011).

The Sérsic fits adopted in this paper are carried out on the F160W imaging data of CANDELS. This corresponds to rest-frame wavelength ranges of $\lambda_{\rm rest} \sim 0.55/0.65/0.9\mu$m for $z \sim 2/1.4/0.8$ systems. A possible concern is that this change in rest-frame wavelength may affect the demographics of the population. While the data at shorter wavelengths in the UDS field have not been analyzed with GALFIT, it is possible to test if this may be an issue using GALFITs on a smaller set of CANDELS F160W data in the GOODS South area, in comparison with published GALFITs on the F850LP ACS GEMS data for the extended Chandra Deep Field South (Häussler et al. 2007). We choose galaxies with $0.4 < z < 0.8$ for this test, where the F850LP data span the same range in rest-frame wavelength as the F160W data for $1.3 < z < 2.2$. For systems with low $n \lesssim 1$, we find a slight tendency for the F160W Sérsic index to exceed the F850LP data (by $\lesssim 0.1$ dex), and for $n \gtrsim 2$ there is no systematic difference between the two sets of Sérsic fits. The scatter around these modest offsets is $\sim$0.2 dex, equivalent to the combined uncertainties of the fits. The fraction of systems with $n > 2.5$ in F850LP (restframe $\sim 0.6\mu$m) is in fact 20% larger than the fraction derived using the F160W imaging (restframe $\sim 1\mu$m), opposite in sign and much smaller than the factor of several observed change in the number of high-n galaxies from $z \sim 2$ to the present day. We conclude that our use of F160W data alone across the $0.6 < z < 2.2$ redshift range is not an important source of systematic error in this analysis.

2.4. *SDSS parameters for the low-redshift comparison sample*

In order to connect with the present-day galaxy population, we use a sample of low-redshift galaxies explored in Bell (2008) from the SDSS Data Release Two (Abazajian et al. 2004), and presented in the NYU Value-Added Galaxy Catalog (Blanton et al. 2005). We use foreground extinction-corrected (Schlegel et al. 1998), k-corrected (Bell et al. 2003)

[5] See http://astro-staff.uibk.ac.at/~m.barden/galapagos/

r-band absolute Petrosian magnitude for the galaxy absolute magnitude (random and systematic uncertainties $\lesssim$ 0.15 mag), and model colors for higher S/N estimates of galaxy color (uncertainties $\lesssim$ 0.05 mag). Following Bell et al. (2003), we have merged this catalog with the Two Micron All-Sky Survey (2MASS; Skrutskie et al. 2006), to facilitate SED fitting and to allow splitting of galaxies by $U-V/V-J$ into quiescent and star-forming populations. Stellar masses and rest-frame colors were estimated from *ugrizJK* photometry using the above stellar population model templates.

Star formation and AGN classifications and estimates of total star formation rate were taken from Brinchmann et al. (2004), using emission line measurements described in Tremonti et al. (2004). Galaxies are classified as star forming, AGN, composites, or are left unclassified (typically because the galaxies lack line emission in their SDSS spectra).

The only source of Sérsic fits for all galaxies in our sample is Blanton et al. (2003)[6]. Blanton et al. (2003) fit the light profile of galaxies in the SDSS, measured in circular apertures, with a seeing-convolved Sérsic (1968) profile for all of the galaxies in the VAGC. The Sérsic fits by Blanton et al. (2003) give values for the Sérsic index, in particular, that are offset from n values determined using 2D galaxy image fits. We have compared the Sérsic indices (and other fit parameters) from Blanton et al. (2003) to fits carried out by van der Wel (2008) on a small subset of galaxies in the NYU VAGC. We find that the Sérsic index estimates are related: $\log_{10} n_{2D} \sim -0.39 + 1.75 \log_{10} n_{\rm NYU\,VAGC}$, with 0.2 dex scatter. Half-light radii show the following correlation: $\log_{10} r_{2D} \sim \log_{10} r_{\rm NYU\,VAGC} - 0.05 + 0.025 n_{2D,\rm new}$, with 0.1 dex scatter, where $n_{2D,\rm new}$ is the estimate of equivalent 2D Sérsic index derived from the NYU VAGC Sérsic index using the above relation. A similar analysis was carried out with completely independent GALFITs by Guo et al. (2009), and importantly the above trends are identical in the case of n, and $\lesssim$ 0.05 dex different in the case of r, to the median offsets as a function of n in their Fig. A1. Recall that the 0.2 dex scatter between the 'rescaled' NYU n values and those of van der Wel (2008) or Guo et al. (2009) (or the 0.1 dex scatter in radii) is comparable to the typical joint uncertainties in any comparison of even unbiased values of n (or r). We conclude that these rescaled NYU n and r values are unbiased, have uncertainties comparable to those determined directly from 2D fits, and are appropriate for connecting the evolution of n and r with the results of 2D fitting for the $z > 0.6$ galaxies.

3. THE EVOLVING RELATIONSHIPS BETWEEN STELLAR MASS, COLOR AND MORPHOLOGY

3.1. *Separating galaxies into quiescent and star forming populations*

We choose to separate galaxies by their star formation activity using two sets of independent diagnostics: mid infrared (or for the SDSS emission line) information, and position on optical–near-infrared color-color diagrams. We use both cuts in this paper; we describe the 24μm-derived cuts first (showing how they relate to rest-frame color cuts) and then show the rest-frame color cuts (showing how they relate to 24μm cuts).

At z>0.6, galaxies are classed in large part according to their 24μm emission properties as an admittedly imperfect proxy for obscured SFR (we use emission-line diagnostics and SFR estimates from Brinchmann et al. 2004 for galaxies from the SDSS). Substantial 24μm flux can also result from AGN activity. We do not attempt to discriminate between AGN activity and SF activity for our purposes here, simply noting that systems with their 24μm flux dominated by AGN at this 24μm luminosity and redshift range are not the dominant population (e.g., Donley et al. 2008; Kartaltepe et al. 2010), and that we are primarily attempting to weed out galaxies whose rest-frame optical colors are a poor reflection of the stellar populations in that galaxy, a goal for which our simple approach is sufficient.

In this spirit, we wish to avoid an explicit, and uncertain, conversion of 24μm flux into SFR (e.g., Papovich et al. 2007; Elbaz et al. 2011; Wuyts et al. 2011a). At each redshift of interest, we fit the relationship between 24μm flux and stellar mass for galaxies detected at 24μm (shown as filled symbols), as shown in Fig. 1. The approximate trend at all redshifts is $\log_{10} f_{24}/\mu{\rm Jy} \sim 2 + 0.5 \log_{10}(M_*/3 \times 10^{10} M_\odot)$, with a scatter of less than 0.3 dex (we use the actual fits and scatters, which vary slightly with redshift, to perform the split into star forming and quiescent). The slope and scatter of this relationship is well-documented and studied (e.g., Salim et al. 2005; Zheng et al. 2007; Noeske et al. 2007; Karim et al. 2011); it is a remarkable coincidence that the zero point in terms of 24μm flux varies so little with redshift, owing to the interplay between the dramatic reduction of SFR at a given stellar mass with decreasing redshift, the luminosity distance and the redshift-dependent 24μm k-correction. Quiescent galaxies then must have a 24μm flux (UDS) or SFR (SDSS) lower than -1σ from the star forming galaxy locus.

In Fig. 1, we have color-coded symbols by their position on the rest-frame $U-V/V-J$ diagram (Fig. 2), using the slightly redshift-dependent cuts described in Williams et al. (2009). Orange symbols show galaxies with rest-frame optical–near-IR colors characteristic of quiescent galaxies, and purple symbols show galaxies with colors characteristic of star-forming galaxies with a range of reddening values. In Fig. 2, we show the optical–near-IR colors of galaxies in the six redshift intervals of interest in this paper. In contrast to Fig. 1, we have color-coded the symbols in Fig. 2 by 24μm flux (UDS) or SFR (SDSS). Galaxies with 24μm fluxes/SFRs lower than -1σ from the star forming galaxy locus have been color-coded red, and galaxies with fluxes/SFRs higher than -1σ from the SF galaxy locus have been color-coded blue. In the $z < 0.05$ slice, emission-line diagnostics are available, and any object with AGN-like lines or composite SF/AGN lines (Brinchmann et al. 2004) have been color-coded green.

Inspection of Figs. 1 and 2 shows the large degree of overlap, and the complementarity of having both explicit 24μm/SFR information and $U-V/V-J$ colors (see also Williams et al. 2009, Wuyts et al. 2009 and Brammer et al. 2011). Galaxies with quiescent $U-V/V-J$ tend, for the most part, to be undetected at 24μm (Fig. 1). There are exceptions to this: a few galaxies with quiescent $U-V/V-J$ at $z \lesssim 1.5$ are detected at 24μm, and by $z \sim 2$ it is clear that for our particular dataset the contamination of the quiescent region of $U-V/V-J$ color space by 24μm-detected objects is significant. Stacking at 24μm of the remaining individually-undetected galaxies with quiescent $U-V/V-J$

[6] Simard et al. (2011) also fit all galaxies in the SDSS with single Sérsic profile fits. We find that for our particular sample half of the fits (those with larger quoted formal uncertainties from Simard et al. 2011, we believe indicative of failed fits) have very large discrepancies compared to fits from Blanton et al. (2003) or van der Wel (2008). Because these poor fits comprise some $\sim 1/2$ of our sample, we cannot adopt the estimates of Simard et al. (2011) for this work.

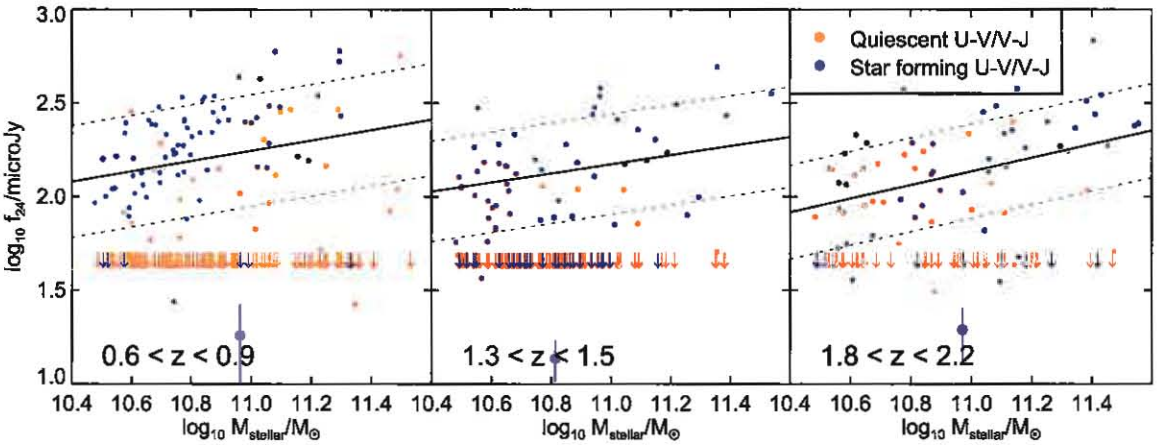

FIG. 1.— Flux at 24μm as a function of stellar mass in three different redshift bins; detections are shown as filled symbols and 4σ upper limits shown by arrows. The thick solid line and dotted lines are the robust linear fits to the data and the $\pm 1\sigma$ range. Colors denote classification according to $U-V/V-J$ (Fig. 2): purple symbols denote galaxies that lie in the star forming part of the color–color diagram, and orange galaxies line in the quiescent region of the plot. The large solid purple points with error bars show the stacked 24μm flux and uncertainty for galaxies individually undetected at 24μm but in the star-forming part of the $U-V/V-J$ diagram.

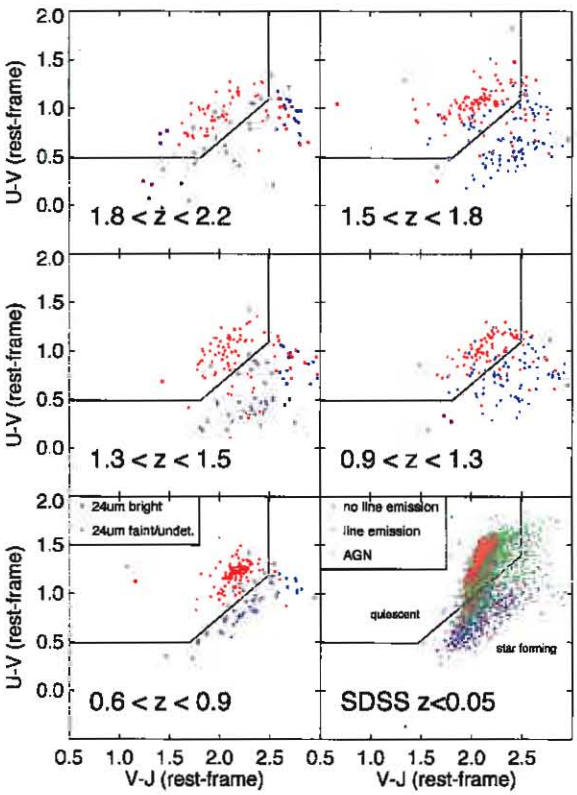

FIG. 2.— Rest-frame $U-V$ as a function of $V-J$ color for the six redshift bins used in this paper. Galaxies are color-coded according to their 24μm properties ($z > 0.6$) or emission line properties ($z < 0.05$); (quiescent) galaxies not detected or fainter than -1σ from the star forming galaxies locus are color-coded red, and the rest of the galaxies (all star forming) are color coded blue. Green galaxies at $z < 0.05$ are galaxies in the SDSS with AGN-like emission lines. Superimposed are the rest-frame color cuts used in this paper, following Williams et al. (2009).

yields marginal (2-3σ significance) detections at the $5-10\mu$Jy level at all redshifts (indicating SF/AGN activity a factor of > 10 lower than typical star-forming galaxies at that redshift; see also Papovich et al. 2006 for an early discussion of star formation in red-selected galaxies).

Conversely, galaxies detected clearly at 24μm are almost always in the star forming region of $U-V/V-J$ (Fig. 2), but again with some exceptions (e.g., at $z \sim 1.4$ there is a clear group of galaxies with star forming colors but are individually undetected at 24μm). Stacks of those few individually 24μm undetected galaxies with star-forming colors yields significant detections at the 15-25μJy level (blue filled points with error bars on Fig. 1), a factor of a few below the SF galaxies locus, largely consistent with an interpretation of these systems as the low SFR tail of the SF galaxy population. This high degree of correspondence between the two methods has been shown before by e.g., Williams et al. (2009) and Wuyts et al. (2009). Fig. 2 also shows that the use of rest-frame color information for $z < 0.05$ is particularly valuable; galaxies classified as AGN can have either quiescent or star forming colors.

We choose to separate galaxies into quiescent and star forming using both criteria, to capitalize on their different strengths and shortcomings. Discrimination by $U-V/V-J$ is sensitive to lower amounts of star formation than 24μm separation, especially at $z \sim 1.4$ and $z \sim 2$. On the other hand, separation by 24μm is considerably less sensitive to photoz error than $U-V/V-J$, as one simply needs to know which redshift bin the galaxy is in, and even some cross-talk between bins can be tolerated. We define quiescent galaxies as having *both* 'quiescent' colors in $U-V/V-J$ and 24μm fluxes/SFRs lower than -1σ from the star forming galaxy locus at the redshift of interest. For SDSS galaxies with AGN-like emission lines, we split only on the basis of $U-V/V-J$. Star forming galaxies are defined as those which satisfy either (or both) of the $U-V/V-J$ star forming galaxy color cuts or having 24μm fluxes/SFRs brighter than -1σ from the star forming galaxy locus. One can see that incorporating 24μm data and insight from $U-V/V-J$ into this analysis is crucial. As can be seen directly in Figs. 1 and 2, and further appreciated by the intermixing of blue and red symbols at red rest-frame $U-V$ in Figs. 3–6, failure to flag galaxies by multiwavelength-derived SF activity leads to considerable confusion between star forming galaxies with substantial dust columns and non star-forming galaxies, especially at higher redshifts (Taylor et al. 2009; Brammer et al. 2011).

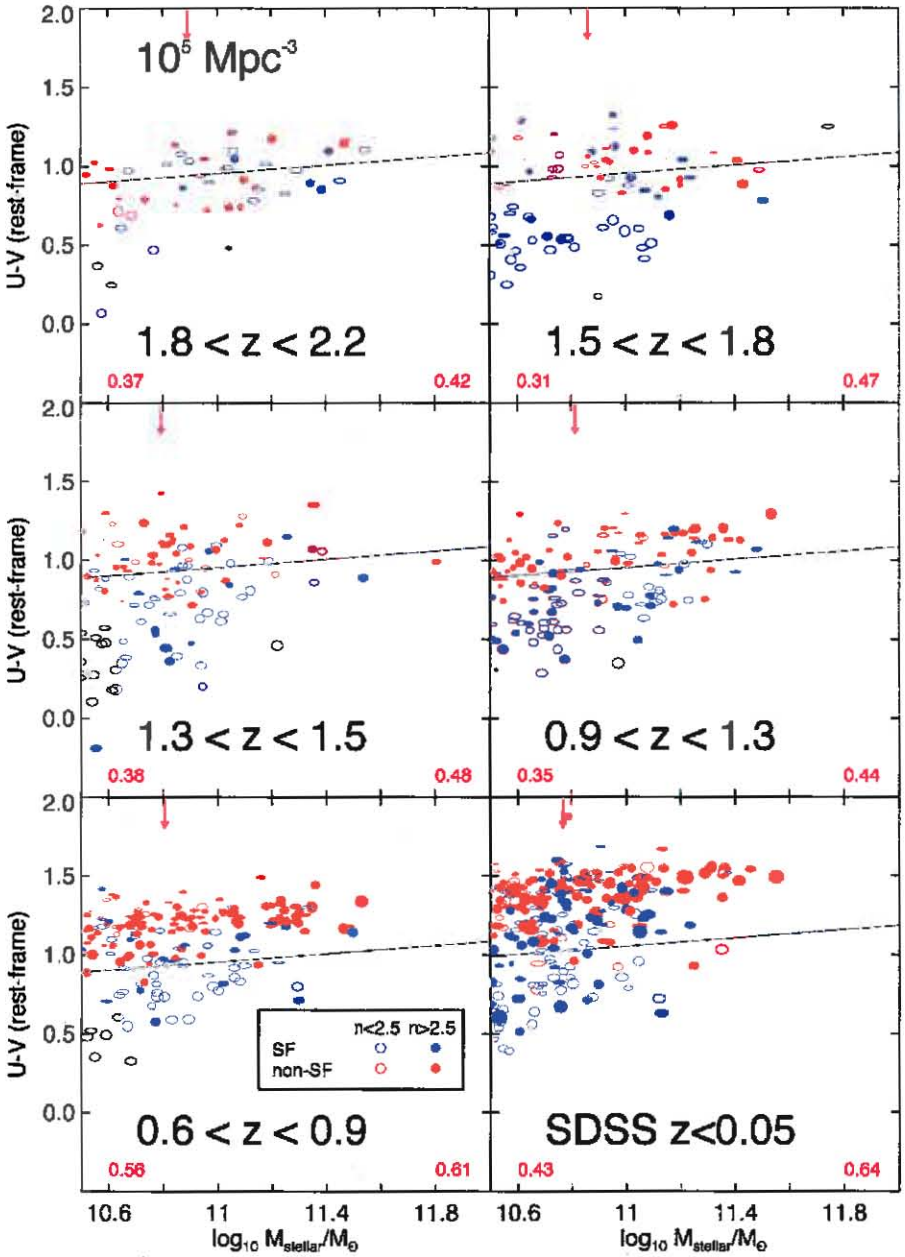

FIG. 3.— The evolution of $U-V$ rest-frame color (in Vega magnitudes) as a function of stellar mass, in six different redshift bins. Galaxies that appear in this figure are subsampled to a volume of 10^5Mpc^3; i.e., this shows the evolution of the massive galaxy content of a 'representative' volume with cosmic time. Open symbols show galaxies with $n < 2.5$ and filled symbols show galaxies with $n > 2.5$. For all symbols the axis ratio of the galaxy is reflected by the axis ratio of the symbol, and the size of the symbol scales with $(1+\log_{10} r_e/\mathrm{kpc})$. The black line is shown in all panels at the approximate locus of $z \sim 2$ red galaxies. Galaxies at $z > 0.6$ are color-coded by star formation activity — galaxies classified as quiescent by both 24μm/SFR and $U-V/V-J$ diagnostics are color-coded red, and blue symbols show galaxies classified as star forming using either $U-V/V-J$ or 24μm/SFR. AGN with $z < 0.05$ are classified using only $U-V/V-J$. In all panels, the small red arrow shows the median mass of the *whole* (not subsampled to 10^5Mpc^3) sample at that redshift, and the small red numbers on the left/right show the fractions of quiescent galaxies in the halves of the *whole* sample with masses below/above that median mass respectively.

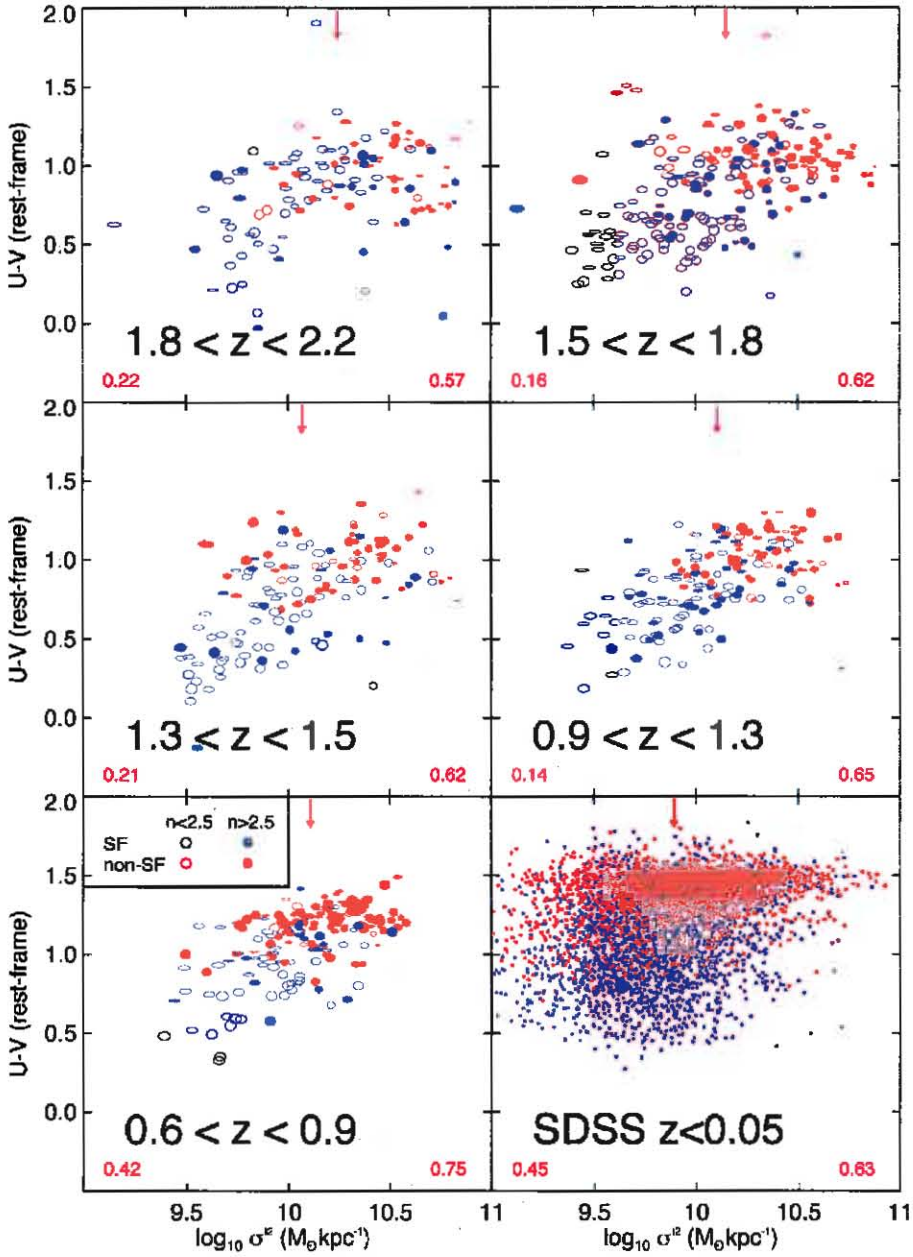

FIG. 4.— The evolution of $U-V$ rest-frame color (in Vega magnitudes) as a function of $0.5M/r_e \sim \sigma'^2$, in six different redshift bins. Symbols are as in Fig. 3 for $z > 0.6$. For the SDSS, we code galaxies only by their star formation activity for clarity. The first five panels ($z > 0.6$) are for the full UDS survey and the SDSS panels use the whole SDSS DR2 subsample used in Bell (2008). In all panels, the small red numbers on the left/right show the fractions of quiescent galaxies in the halves of the sample below and above the median σ' (red arrow), respectively.

3.2. *Evolution of the galaxy population in a given comoving volume*

Fig. 3 shows the rest-frame $U-V$ colors of galaxies, as a function of their stellar mass, in six different redshift bins. We choose to show the properties of the galaxy population as a function of $U-V$ rest-frame color to connect with other studies (e.g., Bell et al. 2004; Borch et al. 2006; Ruhland et al. 2009; Whitaker et al. 2010; Brammer et al. 2011), and as a joint (rather sensitive) constraint on SFH and dust content. Galaxies are color-coded by star formation activity (§3.1): red symbols show galaxies classified as quiescent using both 24μm information and $U-V/V-J$ colors, and blue symbols show the star forming galaxy population. In all panels of this figure, the galaxy population has been Monte Carlo subsampled down to an equivalent volume of 10^5Mpc^3 by adjusting the number of galaxies to track the number density of galaxies with $M_* > 3 \times 10^{10} M_\odot$ determined from larger surveys (the line in Fig. 11). Put differently, variations in the number of galaxies from panel to panel illustrate true evolution in the galaxy population (as the volume is fixed; see Appendix A for further discussion). Filled symbols show galaxies with

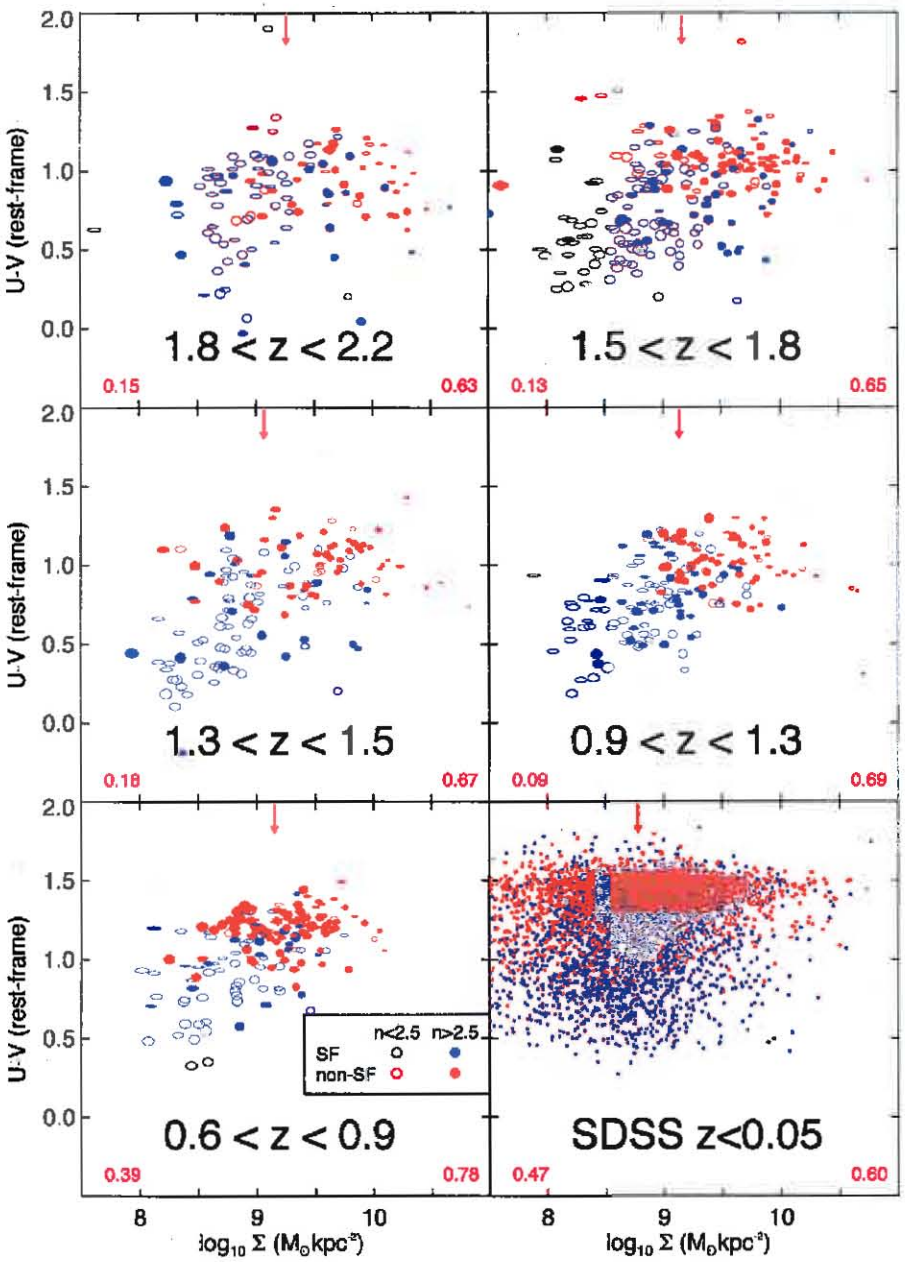

FIG. 5.— The evolution of $U-V$ rest-frame color (in Vega magnitudes) as a function of stellar surface density $0.5M/\pi r_e^2$, in six different redshift bins. The samples and symbols are as in Fig. 4. In all panels, the small red numbers on the left/right show the fractions of quiescent galaxies in the halves of the sample below and above the median stellar surface density (red arrow), respectively.

$n > 2.5$. Open symbols show galaxies with $n < 2.5$. In all panels, the linear size of the symbol scales with $(1+\log_{10} r_e/\mathrm{kpc})$, and the axis ratio of the symbol is the same as that of the galaxy of interest. The black line is shown in all panels, for reference, at the approximate position of $z \sim 2$ non star-forming galaxies.

The evolution of the galaxy population in the epoch $z \sim 2$ to the present day is obvious. As has been argued by a number of other authors (e.g., Arnouts et al. 2007; Fontana et al. 2009; Taylor et al. 2009; Ilbert et al. 2010; Cassata et al. 2011; Domínguez Sánchez et al. 2011; Brammer et al. 2011), there is dramatic evolution in the overall number of galaxies with $M_* > 3 \times 10^{10} M_\odot$ (as quantified in Fig. 11). Furthermore, Fig. 3 shows that the evolution of the number density of quiescent galaxies is particularly striking (again, as has been argued by the above cited works). Fig. 3 makes it clear however that the evolution of the star formation activity of the intermediate-mass and massive galaxy population is accompanied by a large-scale change in the structure of galaxies (see also Wuyts et al. 2011b, who see similar behavior) from a $z \gtrsim 1.5$ population dominated by low n (little or no bulge), mostly star-forming systems to the present population, dominated by galaxies with high n (with a prominent bulge), many of them quiescent (but not all of them). Quantitatively, there

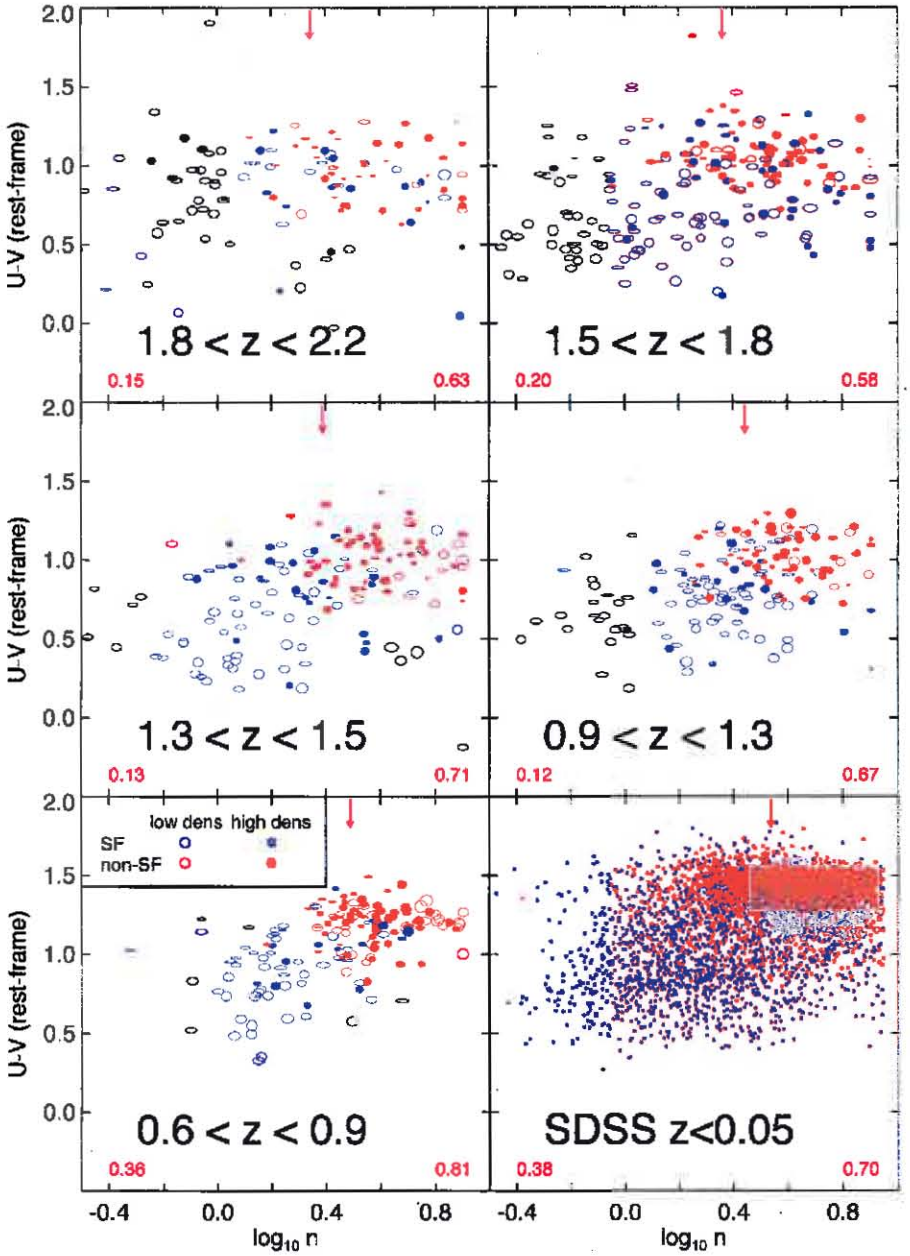

FIG. 6.— The evolution of $U-V$ rest-frame color (in Vega magnitudes) as a function of Sérsic index, in six different redshift bins. The samples and symbols are as in Fig. 4, except that now filled/open symbols denote those galaxies with above/below median surface densities at that redshift (in the stellar mass range considered in this paper). In all panels, the small red numbers on the left/right show the fractions of quiescent galaxies in the halves of the sample below and above the median Sérsic index (red arrow), respectively.

are a factor of ~2.5 (3.5) more quiescent ($n > 2.5$) galaxies with $M_* > 3 \times 10^{10} M_\odot$ today than there were *galaxies* with those masses at $z \sim 2$, respectively. Thinking about it differently, the current population of quiescent ($n > 2.5$) galaxies with $M_* > 3 \times 10^{10} M_\odot$ is approximately as numerous as the entire $M_* > 3 \times 10^{10} M_\odot$ population at $z \sim 1.1$ (0.7) respectively. This change in global demographics from $z \sim 2$ to the present day makes it clear that in addition to processes that shut off star formation on galactic scales, there must be (the same or different) processes that lead to an associated change in the surface brightness profiles of galaxies over the same time period (and given the good correspondence between a lack of star formation and structure, arguably with similar time scales).

Fig. 3 shows also that the scatter in the quiescent galaxy CMR decreases towards lower redshift. The evolution of CMR scatter from $z \sim 2$ to the present day is well-documented in the literature (Ruhland et al. 2009; Whitaker et al. 2010). The scatter in the U-V colors of non star-forming galaxies with $U-V > 0.6$ at $z \geq 1.3$ is 0.17 mag (our measurement), very consistent with the carefully-measured results of Whitaker et al. (2010), who find a scatter of 0.13-0.2 mag for

$1.3 \leq z < 2$. Ruhland et al. (2009) find that the scatter in $U-V$ color at $z \lesssim 1$ is ~ 0.1 mag (measured much more carefully than the CMRs presented in Fig. 3; our measurements also give a scatter of ~ 0.1 mag), essentially independent of redshift. Modeling presented in both Ruhland et al. (2009, for $z < 1$) and Whitaker et al. (2010, at $1 < z < 2$) shows that the evolution of CMR scatter is naturally interpreted as being caused by a constant inflow of new galaxies on to the red sequence at the observed number density growth rate.

4. EMPIRICAL CORRELATIONS BETWEEN A LACK OF STAR FORMATION AND GALAXY STRUCTURE

4.1. *Broad trends*

One of the most notable trends seen by Arnouts et al. (2007), Taylor et al. (2009), Ilbert et al. (2010), Domínguez Sánchez et al. (2011), Brammer et al. (2011) and elaborated upon in Fig. 3 is the dramatic growth of the quiescent galaxy population from $z \sim 2$ to the present day. Fig. 3 demonstrates also that with the growth of the quiescent galaxy population comes a concurrent growth of the population of concentrated $n > 2.5$ galaxies (see also Wuyts et al. 2011b). Franx et al. (2008) argues that these galaxies also have high surface density and 'velocity dispersion', and that 'velocity dispersion' is the parameter that best correlates with a lack of SF activity at $z \lesssim 2$. In this section, we explore how the different structural parameters correlate with star formation activity in an attempt to gain possible insight into the processes that drive galaxies into quiescence.

In Figs. 4 and 5, we show the $U-V$ rest-frame colors of galaxies as a function of $0.5M/r_e \propto \sigma'^2$ (following Franx et al. 2008, where σ' is used to differentiate this quantity from a true velocity dispersion; it should be noted that this quantity also scales with rotation velocity, with a different proportionality constant, for systems dominated by rotation), and $0.5M/\pi r_e^2 = \Sigma$ (surface density within the half-light radius, following Kauffmann et al. 2003, and as explored for low redshift by Bell 2008). Symbols are coded by Sérsic index, axis ratio, size and star formation activity as in Fig. 3. We draw from the full UDS and SDSS DR2 datasets, as opposed to sub-sampling down to an equivalent volume of 10^5Mpc^3, in order to delineate the trends with better fidelity than the subsample shown in Fig. 3.

In Figs. 4 and 5, one can see trends reported by Kauffmann et al. (2003) and Franx et al. (2008): galaxies with either high velocity dispersion, or high surface density, tend not to form stars. Yet, in these figures one can also see the behavior reported by Bell (2008): there are a number of non-star forming galaxies also at low mass, velocity dispersion or surface density, and to a great extent their main defining characteristic is a relatively high Sérsic index[7].

Fig. 6 shows the trend in rest-frame color with Sérsic index. This trend was not explored by Franx et al. (2008), as they did not analyze large-scale HST imaging, and therefore lacked reliable measurements of surface brightness profile shape; this can, however, be compared with (and is consistent with) Fig. 1 of Wuyts et al. (2011b). Symbols are similar to previous figures, except that filled/open symbols now denote galaxies with above/below median stellar surface density at that redshift for the galaxies with $M_* > 10^{10.5} M_\odot$ in our sample (recall that the previous filled/open distinction was by Sérsic index, which would be redundant). Focusing on the $z > 0.6$ points, one can see that galaxies with high Sérsic index are much more likely to be non star-forming than their low Sérsic index counterparts. Furthermore, one can see that there is a range of stellar surface densities at a given Sérsic index. A similar qualitative behavior is seen for the SDSS galaxies, notwithstanding quantitative differences in the definition of Sérsic index for the NYU VAGC catalog. Put differently, the degree of left-right split on the plots between red and blue points (lack of detectable star formation vs. star formation) appears stronger in Fig. 6 than in Figs. 3–5.

4.2. *Which parameter correlates best with a lack of star formation?*

Figs. 3–6 demonstrate that 'typical' quiescent galaxies have higher mass, 'velocity dispersion', surface density and Sérsic index than 'typical' star-forming galaxies. In this section, we will explore further which parameter correlates the best with a lack of star formation activity.

Fig. 7 shows the quiescent fraction (evaluated in running bins of 101 galaxies at $z > 0.6$, or 501 galaxies at $z < 0.05$) as a function of the rank of a galaxy in stellar mass (dotted line), 'velocity dispersion' (grey solid line), surface density (dashed line) and Sérsic index (black solid line) in three broad redshift bins. At all redshifts, stellar mass is a poor predictor of quiescence. At $z < 0.05$, Sérsic index is clearly a better predictor of quiescence than any other parameter; in particular, galaxies with low n overwhelmingly host detectable star formation.

At $0.6 < z < 2.2$, one can see a slightly different situation: 'velocity dispersion', surface density, and Sérsic index correlate comparably well with SF activity. Yet, in both bins, one can see a weaker version of the behavior seen at low redshift: Sérsic index correlates somewhat better with a lack of star formation than either 'velocity dispersion' or surface density. The small numbers on the lower left and right hand corners of each panel of Figs. 3–6 help to illustrate this point. These numbers show the fraction of quiescent galaxies for two different subsamples: the half with lowest stellar M_*, σ', Σ, or n, and the half with highest M_*, σ', Σ, or n. The Sérsic index is the metric that tends maximizes the contrast between the two halves of the sample (except at $0.9 < z < 1.3$ and $1.5 < z < 1.8$, where Sérsic index still correlates very well with quiescence). Note that repeating this analysis with alternate photometric redshifts, stellar masses and rest-frame properties (S. Wuyts et al., in prep.) yields a slightly stronger preference still for n as the parameter that best correlates with quiescence.

Fig. 8 emphasizes this finding. In the same three broad redshift bins, we show $U-V$ color of galaxies as a function of 'velocity dispersion' (found by Franx et al. 2008 and E. Cheung et al., in prep., to correlate marginally better with a lack of star formation than surface density). Symbols are coded as they are in Figs. 3–5. The top panels show galaxies with $n < 1.5$ (galaxies with little or no bulge) and the bottom panels show galaxies with $n > 3$ (galaxies with a prominent bulge). The population with $n < 1.5$ is overwhelmingly star forming. In strong contrast, the $n > 3$ population has a large quiescent fraction. Strikingly, one can see that star formation or quiescence happens over a wide range in 'velocity dispersion'.

There are two emergent themes that we wish to draw the reader's attention to. First, Figs. 6 and 8 show that, with very

[7] The actual fraction of galaxies forming stars at low Σ or σ' may be rather higher, as the sample is limited by stellar mass. Fig. 3 shows that quiescent galaxies are smaller at a given stellar mass than star-forming galaxies, therefore it is possible that if Figs. 4 and 5 were σ' or Σ limited samples they would show a more prominent population of (lower stellar mass) quiescent galaxies with relatively low σ' or Σ.

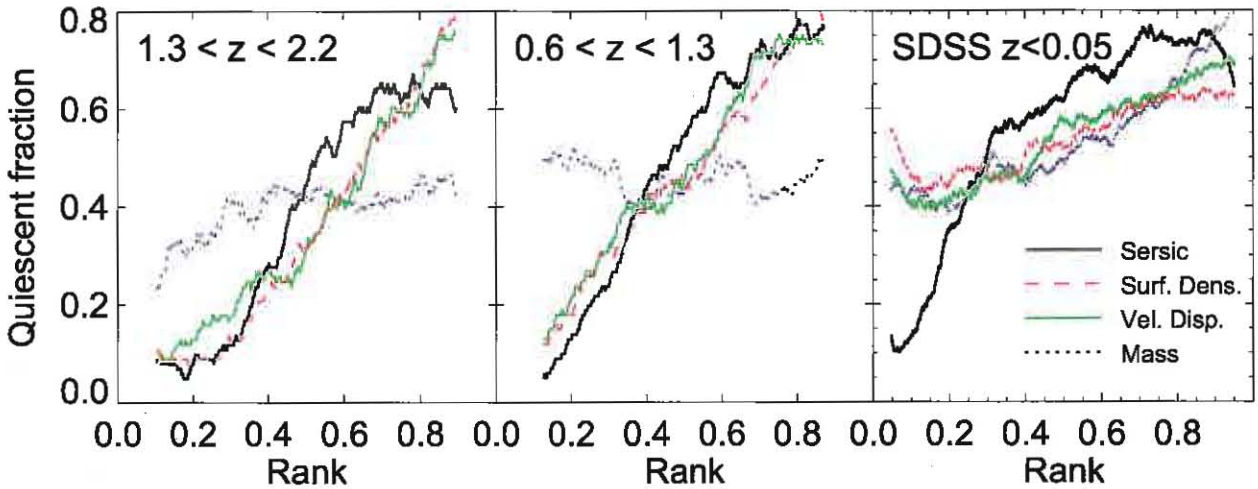

FIG. 7.— The quiescent fraction in three broad redshift bins as a function of the rank of n, Σ, σ', and M_* (rank denoting where a galaxy is in the sorted list of the n, σ' or M_* in the sample at that redshift of interest). These are running average fractions determined for the ± 50 (250 for the SDSS) nearest neighbors in rank of the quantity in question. Mass is always a poor predictor of quiescence; Sérsic index is clearly superior to Σ or σ' at $z < 0.05$, and performs as a slightly better predictor of quiescence for all $z < 2.2$.

few exceptions, galaxies with low Sérsic index all appear to form stars at all $z \lesssim 2.2$. The threshold appears to be somewhere around $n \sim 1.5-2$: at $n \lesssim 2$, the fraction of quiescent galaxies is $\lesssim 10\%$ (and in many redshift bins it is less than a few percent). When investigated in more detail using the same SDSS sample (Bell 2008), it was found that i) real low n quiescent galaxies are all satellite galaxies in galaxy clusters, i.e., they are stripped disk galaxies, and ii) the few quiescent 'low n' systems in the centers of their own halos that remained were in fact the result of measurement error in n, as visual inspection showed a distinct bulge component. We show examples of some $n < 2$ quiescent galaxies at $z > 1.5$ in Fig. 9 (at $0.9 < z < 1.5$ there are only three $n < 2$ quiescent systems, and those look similar to the $z > 1.5$ examples; the $0.6 < z < 0.9$ points are bad Sérsic fits). While some systems are relatively extended and have low n, and the one inclined galaxy is clearly reminiscent of a disk, most appear spheroidal and compact. Given Figs. 6 and 9 in concert, it is clear the vast majority of quiescent galaxies have a prominent spheroid. This extends the results of Bell (2008) determined for nearby galaxies to $z \sim 2.2$, when the Universe was $\sim 1/4$ of its present age: galaxies lacking a prominent bulge appear to have great difficulty shutting off their own star formation on galactic scales.

Second, Figs. 6 and 8 make it clear that having a high Sérsic index alone (or indeed, having high n, σ', Σ and M_*) is not enough to ensure a lack of star formation. At all redshifts, a small minority of high n sources form stars at an appreciable rate. This illustrates a key point of this paper; it appears that for all $z \lesssim 2.2$, a large bulge is *necessary* to stop star formation, but is not *sufficient* to stop star formation. This extends the conclusion of Bell (2008) determined for local galaxies out to $z \sim 2.2$, when the non star-forming galaxy population was considerably less prominent.

5. DISCUSSION

There are two main observational results in this paper: the rapid growth of the quiescent galaxy population between $z = 2$ and the present day, and the recognition that this growth appears to be intimately linked to the growth of the high Sérsic index galaxy population.

5.1. *Musings on the mechanisms that prevent significant cold gas in galaxies*

These results have some bearing on understanding which mechanisms lead to quenching of star formation in galaxies. Recall that the role of environmental quenching is relatively minor in our 'cosmic averaged' population evolution, and that we are focusing on which types of physical process lead to quenching of star formation in galaxies in the centers of their halos (the mass quenching of Peng et al. 2010). To facilitate this, we will set up two straw person hypotheses: suppression of star formation by feedback (either star formation or AGN feedback; 'feedback quenching', e.g., Kauffmann & Haehnelt 2000, Croton et al. 2006, Somerville et al. 2008), or suppression of star formation because the halo reaches a certain critical mass ('halo quenching'; e.g., Dekel & Birnboim 2006, Cattaneo et al. 2006).

Fig. 7 demonstrates that internal properties (Sérsic index, and to a lesser extent 'velocity dispersion' and surface density) correlate strongly with quiescence, whereas galaxy mass only weakly correlates with star formation activity. Galaxy mass is expected to correlate well with halo mass. More et al. (2009) measure the scatter in luminosity at a given halo mass to be 0.16 dex, substantially less than the $\sim$ 1dex dynamic range probed in this work. The observed weakness of correlation between quiescent fraction with stellar mass, coupled with the expected modest scatter between stellar mass (via its proxy, luminosity) and halo mass, implies a weak correlation between halo mass and quiescence at all $z < 2.2$. This is consistent with the claim by More et al. (2011) that at fixed stellar mass there is *no difference* between the average halo masses of quiescent and star-forming central galaxies. We conclude that quiescence is not determined by halo mass *alone*.

The results here demonstrate that systems with high Sérsic index, and to a certain extent systems with high 'velocity dispersion' and high surface density, are much more likely to be quiescent (see also Franx et al. 2008 and Wuyts et al. 2011b). In the context of gas expulsion (or prevention of cooling) by feedback, it is suggestive that the best correlation with

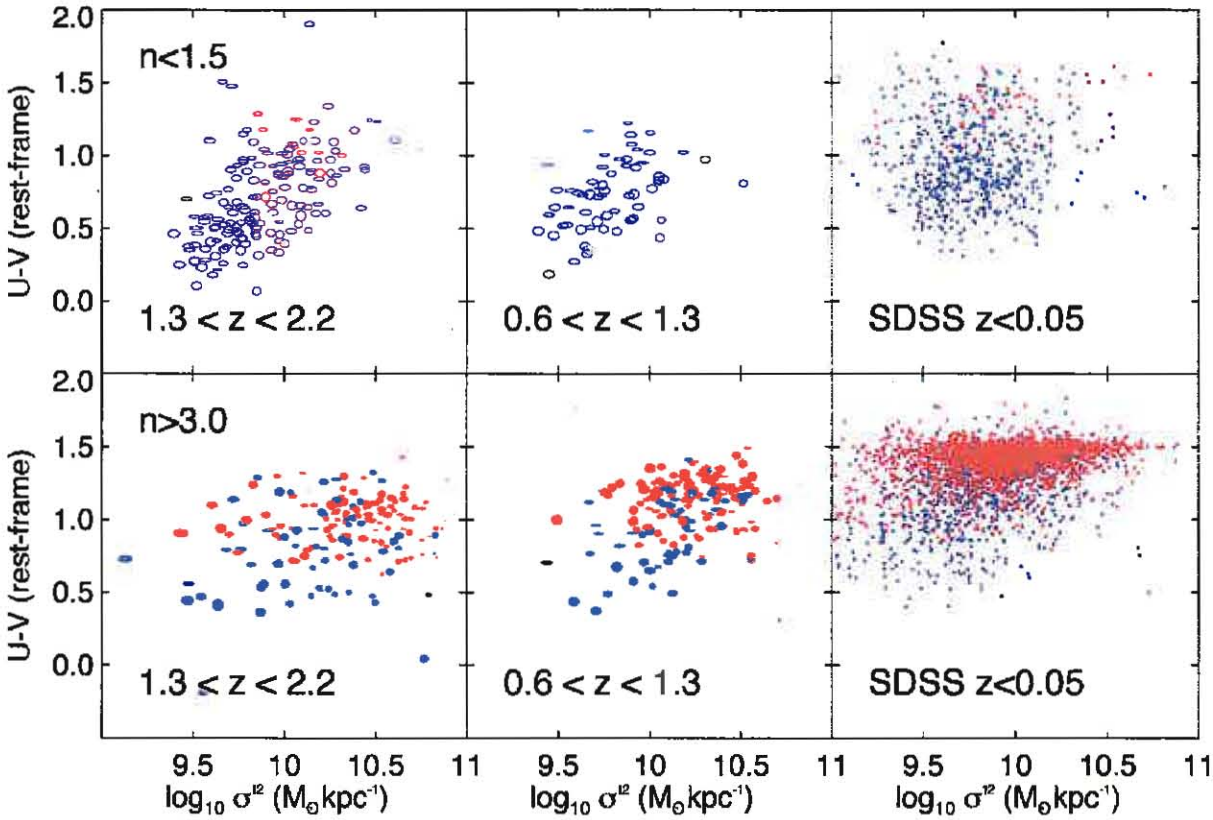

FIG. 8.— The evolution of $U-V$ rest-frame color (in Vega magnitudes) as a function of $0.5M/r_e \sim \sigma'^2$, in three broad redshift bins. The top panels show galaxies with $n < 1.5$ (galaxies with little or no bulge), the bottom panels show only galaxies with $n > 3$ (galaxies with a prominent bulge component). Symbols are as in Fig. 4. A lack of star formation (red symbols) can happen over a wide range in σ', but correlates strongly with n.

quiescence is Sérsic index (an imperfect proxy for the relative prominence of a bulge component). Given the black hole mass–bulge mass correlation (Häring & Rix 2004; Peng et al. 2006; Gültekin et al. 2009), our results tentatively support the AGN feedback paradigm, at least at the qualitative level. In particular, the seeming inability of galaxies with low Sérsic indices to shut off their star formation is very naturally interpreted in this framework (Bell 2008) — no supermassive black hole, no shut-off of star formation. We note that feedback from star formation-driven winds may also be of relevance, but we caution that the results shown here argue that such winds must be efficient at wholesale ISM removal *only* during star formation events that create a prominent bulge (as disk galaxies keep forming stars with enthusiasm).

5.2. *Quiescent disks?*

There has been much recent discussion of the presence and importance of stellar disks in quiescent galaxies. At $z \gtrsim 1.5$, Stockton et al. (2004), McGrath et al. (2008), van Dokkum et al. (2008) and van der Wel et al. (2011) have argued that most quiescent galaxies with masses in excess of $10^{11} M_\odot$ have prominent stellar disks. Bundy et al. (2010) has explored this issue at $z < 1.2$, finding that a large fraction of quiescent galaxies have disks in addition to significant bulge components; indeed, the existence of S0s and disky ellipticals in all environments is well-known (see, e.g., van den Bergh 2009, and references therein). The highly-inclined fraction of these systems are clearly visible in Fig. 6, as the elongated

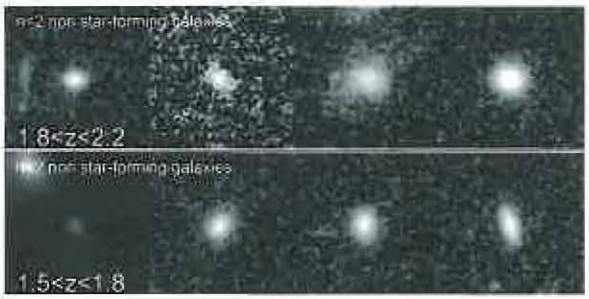

FIG. 9.— F160W Postage stamps of quiescent galaxies with $n < 2$ and stellar surface densities between 10^9 and $10^{10} M_\odot$ kpc^{-2}. The postage stamps, within each class, are ordered by stellar mass (ordered left to right). At all redshifts, all postage stamps are 40 physical kpc on a side, and are scaled to a constant 'stellar mass density' (total intensity is scaled to total stellar mass, meaning that if the stellar M/L is constant over the face of the galaxy this postage stamp should reflect the stellar mass density) and are displayed using asinh scaling (linear at low intensity, and logarithmic at higher surface brightness; Lupton et al. 1999).

symbols with low b/a. Such systems appear to be somewhat more common at $z > 1.5$, but are present (especially at lower Sérsic indices $n \sim 2-3$) at all redshifts.

There are two comments that we wish to make about this issue. Firstly, the vast majority of these systems have Sérsic indices $n \gtrsim 2$. In McGrath et al. (2008) and van der Wel et al. (2011), bulge/disk decompositions were carried out, and showed that these systems with relatively high Sérsic index are also well-explained as composite bulge/disk systems

with relatively large bulges. Furthermore, kinematic studies of local quiescent galaxies has demonstrated that the vast majority of quiescent galaxies have significant rotation (Emsellem et al. 2011), and the incidence of strong rotation signatures in quiescent galaxies does not change from $z \sim 1$ to the present day (at $\sim 60\%$, van der Wel & van der Marel 2008). The picture that emerges here is that the vast majority of quiescent systems have undergone some event that both steepens their light profile (either by creation of a distinct bulge component, or simply by steepening the light profile) but manages to retain a significant fraction of the system's original angular momentum in preserving a disk component. In the context of galaxy merging, such systems are a relatively natural outcome of merging between disk galaxies with even modest gas fractions, where higher mass ratio minor mergers (or mergers between more gas-rich systems) lead to are progressively more disk-dominated remnants (see, e.g., Naab et al. 2006, Hopkins et al. 2009, Hoffman et al. 2010).

Secondly, a small fraction of quiescent systems appear to have little in the way of a bulge component (Bell 2008; Stockton et al. 2004; McGrath et al. 2008; Bundy et al. 2010); the examples in McGrath et al. (2008) have been very carefully documented. At least a few of the examples in Fig. 9 appear to have genuinely low-concentration light profiles, and at least one is an inclined disk. Given that such systems in the local universe appear to all be satellites in high mass (group or cluster) halos (Bell 2008), it will be interesting to explore the environments of such galaxies, as a function of redshift, and help to elucidate the extent to which disk-only quiescent galaxies are the products of stripping of their cold gas content by hot gas in a deep potential well (in this context, it is worth noting that the $z \sim 1.5$ systems in McGrath et al. 2008 were chosen to be in fields near radio-loud $z \sim 1.5$ QSOs, and may in fact reside in overdensities).

5.3. *On the nature of high Sérsic index star-forming galaxies*

Figs. 6 and 8 show a population of star-forming galaxies with high Sérsic index. We show examples of such systems in Fig. 10 in 5 different redshift bins. One can see that these high Sérsic index, star-forming systems fall broadly into two types of systems. At lower redshifts, there are some clear examples of disks with very prominent bulges; such galaxies are the star-forming counterparts of the quiescent disks discussed above, and appear to be systems that have either retained, or 're-grown', a substantial disk during/after a bulge formation event (Baugh et al. 1996; Kannappan et al. 2009; Benson & Devereux 2010). At all redshifts, there are what appear to be genuinely spheroidal galaxies, but in many cases with significant asymmetries, and in some cases evidence of interactions (e.g., nearby companions, tidal tails). It will be interesting to examine such systems in the future to understand the degree of overlap between these systems and 'blue spheroids' (Menanteau et al. 2001; Häußler 2007; Kannappan et al. 2009; Győry & Bell 2010), post-starburst galaxies (Vergani et al. 2010), or ongoing 'bulge-building' starbursts (Wuyts et al. 2011b) and to ask if the properties of these galaxies are more consistent with an interpretation as a quiescent galaxy in formation, or a galaxy in the early stages of re-growing a disk (Kannappan et al. 2009).

5.4. *Future steps*

There are a number of possible future directions for pursuing this line of study further. Sharpening the analysis would be possible with the addition of reliable bulge/disk decompositions: the hypothesis that the existence of a prominent bulge is necessary but not sufficient to shut off star formation can be better tested, and additional parameters can be explored for possible relevance (e.g., bulge/total ratio, bulge Sérsic index, or bulge mass; see, e.g., Drory & Fisher 2007 for an exploration of some of these issues with a low-redshift sample). More detailed exploration of the outliers at all redshifts (the quiescent lower Sérsic index systems, or star-forming systems with high Sérsic index) may help to illuminate the processes that remove (or keep out) cold gas from galaxies. Finally, increasing the number statistics at $z < 1$ (already underway with, e.g., the GEMS, AEGIS or COSMOS datasets; Rix et al. 2004, Davis et al. 2007, Scoville et al. 2007) and at $z > 1$ with the full five field coverage of CANDELS (Grogin et al. 2011; Koekemoer et al. 2011) may prove useful.

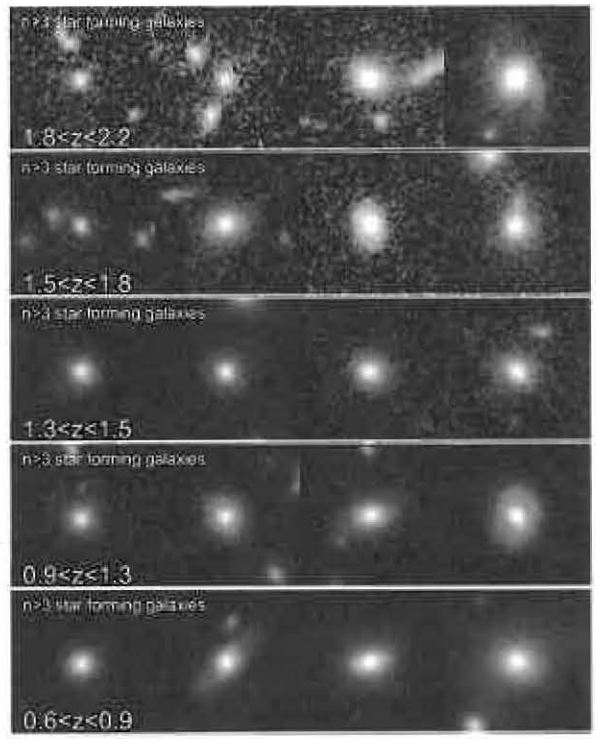

FIG. 10.— F160W Postage stamps of star-forming galaxies with $n > 3$ and stellar surface densities between 10^9 and $10^{10} M_\odot\,\mathrm{kpc}^{-2}$. The postage stamps, within each class, are ordered by stellar mass (ordered left to right). At all redshifts, all postage stamps are 40 physical kpc on a side, and are scaled to a constant 'stellar mass density' (total intensity is scaled to total stellar mass, meaning that if the stellar M/L is constant over the face of the galaxy this postage stamp should reflect the stellar mass density) and are displayed using asinh scaling (linear at low intensity, and logarithmic at higher surface brightness; Lupton et al. 1999).

6. CONCLUSIONS

Motivated by a desire to empirically explore the evolutionary factors that lead to a lack of star formation in galaxies, we have explored the structures and star formation activity of the galaxy population using the HST/WFC3 F160W imaging data from CANDELS in the UDS field. We used public photometry and photometric redshifts from Williams et al. (2009), and determined rest-frame absolute magnitudes and stellar masses using our own stellar population model fits. We supplement this with public 24μm data from SpUDS, and separate galaxies into quiescent and star-forming using a combi-

nation of optical–near-infrared colors and 24μm information. For structural information, we use parametric fits of a single Sérsic profile to the WFC3 F160W imaging data. We then combine these data for $z > 0.6$ galaxies with a sample with similar parameters from the SDSS, to create a $z < 0.05$ comparison sample. We then proceed to explore the evolution of the $M_* > 3 \times 10^{10} M_\odot$ galaxy population from $z = 2.2$ to the present day.

We first visualize the evolution of the galaxy population over the last 10 Gyr by normalizing the sample to a 'fixed' comoving volume of 10^5 Mpc^3. In agreement with a large number of other works, we find that the number density of massive galaxies increases approximately five-fold from $z \sim 2$ to the present day, and that the number density of quiescent galaxies increases yet more rapidly. Furthermore, examining the properties of the quiescent galaxy population, we find that the vast majority of those quiescent galaxies have high Sérsic indices, a sign that they have a prominent bulge component. The growth of the quiescent galaxy population appears to be intimately linked with the growth of the high Sérsic index population.

Given the rapid evolution of the quiescent galaxy population, we proceed to explore the strength of the correlation between quiescence and four galaxy/structural parameters: stellar mass, 'velocity dispersion' $M/R \propto \sigma'^2$, stellar surface density and Sérsic index. At all redshifts $z < 2.2$, stellar mass correlates poorly with quiescence. Bearing in mind the $\lesssim 0.2$ dex scatter between stellar mass and dark matter halo mass at $z \sim 0$, this argues against the notion that halo mass *alone* is the main determinant of quiescence.

At $z \lesssim 0.05$, we find that Sérsic index correlates much more strongly with quiescence than either velocity dispersion or surface density. At $z \geq 0.6$, we find that velocity dispersion, surface density and Sérsic index correlate well with quiescence, where the correlation of Sérsic index with quiescence is marginally stronger.

All correlations have substantial scatter, however. Many quiescent systems have prominent disks, although the vast majority of quiescent galaxies with disks have prominent bulges. A very small fraction of quiescent galaxies appear to be disk-dominated; in the local Universe they are all satellite galaxies in galaxy groups/clusters, at higher redshifts we did not explore environmental variables for lack of dynamic range in galaxy environments. Star-forming systems with high n, M, Σ and σ' are not particularly uncommon; at high redshifts they appear to be genuinely compact with high n, and often show asymmetries or signatures of tidal interactions (one may wish to associate these with the possible remnants of gas-rich dissipational galaxy interactions/mergers), and at lower redshifts there is a mix of similar systems and composite bulge-disk star-forming systems (with large bulges).

At $z < 0.05$, Bell (2008) concluded that a prominent bulge (and by association, a supermassive black hole) was a necessary but not sufficient condition for a galaxy to turn off its own star formation on galaxy-wide scales (all quiescent galaxies in the centers of their own halos had prominent bulges, but not all galaxies with bulges lack star formation). This observational association is qualitatively consistent with the AGN feedback paradigm (no supermassive black hole, no ability to shut off star formation). While there is clearly scope for further investigation of the drivers of quiescence, the evidence assembled here appears to be consistent with this proposition to $z < 2.2$, a time interval of more than 10Gyr.

This work is supported by HST grant GO-12060. Support for Program number GO-12060 was provided by NASA through a grant from the Space Telescope Science Institute, which is operated by the Association of Universities for Research in Astronomy, Incorporated, under NASA contract NAS5-26555.

This publication makes use of the *Sloan Digital Sky Survey* (SDSS). Funding for the creation and distribution of the SDSS Archive has been provided by the Alfred P. Sloan Foundation, the Participating Institutions, the National Aeronautics and Space Administration, the National Science Foundation, the US Department of Energy, the Japanese Monbukagakusho, and the Max Planck Society. The SDSS Web site is `http://www.sdss.org/`. The SDSS Participating Institutions are the University of Chicago, Fermilab, the Institute for Advanced Study, the Japan Participation Group, the Johns Hopkins University, the Max Planck Institut für Astronomie, the Max Planck Institut für Astrophysik, New Mexico State University, Princeton University, the United States Naval Observatory, and the University of Washington. This publication also makes use of data products from the Two Micron All Sky Survey, which is a joint project of the University of Massachusetts and the Infrared Processing and Analysis Center/California Institute of Technology, funded by the National Aeronautics and Space Administration and the National Science Foundation. This publication also made use of NASA's Astrophysics Data System Bibliographic Services.

REFERENCES

Abazajian, K., et al. 2004, AJ, 128, 502
Arnouts, S., et al. 2007, A&A, 476, 137
Barnes, J. E., & Hernquist, L. 1992, ARA&A, 30, 705
Baugh, C. M., Cole, S., & Frenk, C. S. 1996, MNRAS, 283, 1361
Bell, E. F. 2008, ApJ, 682, 355
Bell, E. F., & de Jong, R. S. 2001, ApJ, 550, 212
Bell, E. F., McIntosh, D. H., Katz, N., & Weinberg, M. D. 2003, ApJS, 149, 289
Bell, E. F., et al. 2004, ApJ, 608, 752
Bell, E. F., Zheng, X. Z., Papovich, C., Borch, A., Wolf, C., & Meisenheimer, K. 2007, ApJ, 663, 834
Benson, A. J., Bower, R. G., Frenk, C. S., Lacey, C. G., Baugh, C. M., & Cole, S. 2003, ApJ, 599, 38
Benson, A. J., & Devereux, N. 2010, MNRAS, 402, 2321
Best, P. N., Kaiser, C. R., Heckman, T. M., & Kauffmann, G. 2006, MNRAS, 368, L67
Birnboim, Y., Dekel, A., & Neistein, E. 2007, MNRAS, 380, 339
Blanton, M. R., et al. 2005, AJ, 129, 2562
Blanton, M. R., Hogg, D. W., Bahcall, N. A., & et al. 2003, ApJ, 594, 186
Borch, A., et al. 2006, A&A, 453, 869
Brammer, G. B., van Dokkum, P. G., & Coppi, P. 2008, ApJ, 686, 1503
Brammer, G. B., et al. 2011, ApJ, 739, 24
Brinchmann, J., Charlot, S., White, S. D. M., Tremonti, C., Kauffmann, G., Heckman, T., & Brinkmann, J. 2004, MNRAS, 351, 1151
Brown, M. J. I., Dey, A., Jannuzi, B. T., Brand, K., Benson, A. J., Brodwin, M., Croton, D. J., & Eisenhardt, P. R. 2007, ApJ, 654, 858
Bruzual, G., & Charlot, S. 2003, MNRAS, 344, 1000
Bundy, K., et al. 2010, ApJ, 719, 1969
Calzetti, D. 2001, PASP, 113, 1449
Cameron, E., Carollo, C. M., Oesch, P. A., Bouwens, R. J., Illingworth, G. D., Trenti, M., Labbé, I., & Magee, D. 2010, arXiv:1007.2422
Cassata, P., et al. 2011, arXiv:1106.4308
Cattaneo, A., Dekel, A., Devriendt, J., Guiderdoni, B., & Blaizot, J. 2006, MNRAS, 370, 1651
Chabrier, G. 2003, PASP, 115, 763
Croton, D. J., et al. 2006, MNRAS, 365, 11

Davé, R., Oppenheimer, B. D., & Finlator, K. 2011, MNRAS, 867
Davis, M., et al. 2007, ApJ, 660, L1
Dekel, A., & Birnboim, Y. 2006, MNRAS, 368, 2
—. 2008, MNRAS, 383, 119
Domínguez Sánchez, H., et al. 2011, arXiv:1106.3194
Donley, J. L., Rieke, G. H., Pérez-González, P. G., & Barro, G. 2008, ApJ, 687, 111
Drory, N., & Fisher, D. B. 2007, ApJ, 664, 640
Dunne, L., et al. 2009, MNRAS, 394, 3
Elbaz, D., et al. 2011, arXiv:1105.2537
Emsellem, E., et al. 2011, MNRAS, 414, 888
Faber, S. M., et al. 2007, ApJ, 665, 265
Fabian, A. C., Sanders, J. S., Taylor, G. B., Allen, S. W., Crawford, C. S., Johnstone, R. M., & Iwasawa, K. 2006, MNRAS, 366, 417
Fioc, M., & Rocca-Volmerange, B. 1997, A&A, 326, 950
Fontana, A., et al. 2009, A&A, 501, 15
Franx, M., van Dokkum, P. G., Schreiber, N. M. F., Wuyts, S., Labbé, I., & Toft, S. 2008, ApJ, 688, 770
Furusawa, H., et al. 2008, ApJS, 176, 1
Grogin, et al. 2011, arXiv:1105.3753
Gültekin, K., et al. 2009, ApJ, 698, 198
Guo, F., & Oh, S. P. 2008, MNRAS, 384, 251
Guo, Y., et al. 2009, MNRAS, 398, 1129
Győry, Z., & Bell, E. F. 2010, ApJ, 724, 694
Häring, N., & Rix, H.-W. 2004, ApJ, 604, L89
Häußler, B. 2007, PhD thesis, Max-Planck-Institut für Astronomie, Heidelberg, Germany
Häussler, B., et al. 2007, ApJS, 172, 615
Hernquist, L. 1993, ApJ, 409, 548
Hoffman, L., Cox, T. J., Dutta, S., & Hernquist, L. 2010, ApJ, 723, 818
Hopkins, P. F., et al. 2010, ApJ, 715, 202
Hopkins, P. F., Cox, T. J., Dutta, S. N., Hernquist, L., Kormendy, J., & Lauer, T. R. 2009, ApJS, 181, 135
Ilbert, O., et al. 2010, ApJ, 709, 644
Johansson, P. H., Naab, T., & Ostriker, J. P. 2009, ApJ, 697, L38
Kannappan, S. J., Guie, J. M., & Baker, A. J. 2009, AJ, 138, 579
Karim, A., et al. 2011, ApJ, 730, 61
Kartaltepe, J. S., et al. 2010, ApJ, 709, 572
Kauffmann, G., & Haehnelt, M. 2000, MNRAS, 311, 576
Kauffmann, G., et al. 2003, MNRAS, 341, 54
Kereš, D., Katz, N., Weinberg, D. H., & Davé, R. 2005, MNRAS, 363, 2
Khochfar, S., & Ostriker, J. P. 2007, ArXiv e-prints, 704
Koekemoer, A. M., et al. 2011, arXiv:1105.3754
Kriek, M., et al. 2010, ApJ, 722, L64
Kriek, M., van Dokkum, P. G., Franx, M., Illingworth, G. D., & Magee, D. K. 2009, ApJ, 705, L71
Kron, R. G. 1980, ApJS, 43, 305
Lawrence, A., et al. 2007, MNRAS, 379, 1599
Lee, S.-K., Ferguson, H. C., Somerville, R. S., Wiklind, T., & Giavalisco, M. 2010, ApJ, 725, 1644
Lonsdale, C. J., et al. 2003, PASP, 115, 897
Lupton, R. H., Gunn, J. E., & Szalay, A. S. 1999, AJ, 118, 1406
Magorrian, J., et al. 1998, AJ, 115, 2285
Maraston, C. 2005, MNRAS, 362, 799
Maraston, C., Pforr, J., Renzini, A., Daddi, E., Dickinson, M., Cimatti, A., & Tonini, C. 2010, MNRAS, 407, 830
McGrath, E. J., Stockton, A., Canalizo, G., Iye, M., & Maihara, T. 2008, ApJ, 682, 303
Menanteau, F., Abraham, R. G., & Ellis, R. S. 2001, MNRAS, 322, 1
More, S., van den Bosch, F. C., Cacciato, M., Mo, H. J., Yang, X., & Li, R. 2009, MNRAS, 392, 801
More, S., van den Bosch, F. C., Cacciato, M., Skibba, R., Mo, H. J., & Yang, X. 2011, MNRAS, 410, 210
Moster, B. P., Somerville, R. S., Newman, J. A., & Rix, H.-W. 2011, ApJ, 731, 113
Naab, T., Jesseit, R., & Burkert, A. 2006, MNRAS, 372, 839
Naab, T., Johansson, P. H., Ostriker, J. P., & Efstathiou, G. 2007, ApJ, 658, 710
Noeske, K. G., et al. 2007, ApJ, 660, L43
Pannella, M., et al. 2009, ApJ, 701, 787
Papovich, C., et al. 2006, ApJ, 640, 92
Papovich, C., et al. 2007, ApJ, 668, 45
Papovich, C., et al. 2011, submitted to ApJ
Peng, C. Y., Ho, L. C., Impey, C. D., & Rix, H.-W. 2002, AJ, 124, 266
Peng, C. Y., Impey, C. D., Rix, H.-W., Kochanek, C. S., Keeton, C. R., Falco, E. E., Lehár, J., & McLeod, B. A. 2006, ApJ, 649, 616
Peng, Y., Lilly, S. J., Renzini, A., & Carollo, M. 2011, arXiv:1106.2546
Peng, Y.-J., et al. 2010, ApJ, 721, 193
Prochaska, J. X., & Hennawi, J. F. 2009, ApJ, 690, 1558
Rix, H.-W., et al. 2004, ApJS, 152, 163
Robaina, A. R., Bell, E. F., van der Wel, A., Somerville, R. S., Skelton, R. E., McIntosh, D. H., Meisenheimer, K., & Wolf, C. 2010, ApJ, 719, 844
Ruhland, C., Bell, E. F., Häußler, B., Taylor, E. N., Barden, M., & McIntosh, D. H. 2009, ApJ, 695, 1058
Salim, S., et al. 2005, ApJ, 619, L39
Salim, S., et al. 2007, ApJS, 173, 267
Schlegel, D. J., Finkbeiner, D. P., & Davis, M. 1998, ApJ, 500, 525
Schweizer, F., & Seitzer, P. 1992, AJ, 104, 1039
Scoville, N., et al. 2007, ApJS, 172, 1
Sérsic, J. L. 1968, Atlas de galaxias australes (Cordoba, Argentina: Observatorio Astronomico, 1968)
Simard, L., Mendel, J. T., Patton, D. R., Ellison, S. L., & McConnachie, A. W. 2011, ArXiv e-prints
Skrutskie, M. F., et al. 2006, AJ, 131, 1163
Somerville, R. S., Hopkins, P. F., Cox, T. J., Robertson, B. E., & Hernquist, L. 2008, MNRAS, 391, 481
Somerville, R. S., Lee, K., Ferguson, H. C., Gardner, J. P., Moustakas, L. A., & Giavalisco, M. 2004, ApJ, 600, L171
Springel, V., Di Matteo, T., & Hernquist, L. 2005, ApJ, 620, L79
Stockton, A., Canalizo, G., & Maihara, T. 2004, ApJ, 605, 37
Strateva, I., et al. 2001, AJ, 122, 1861
Szomoru, D., Franx, M., Bouwens, R. J., van Dokkum, P. G., Labbe, I., Illingworth, G. D., & Trenti, M. 2011, ApJ, 734, L22
Tal, T., van Dokkum, P. G., Nelan, J., & Bezanson, R. 2009, AJ, 138, 1417
Taylor, E. N., et al. 2009, ApJS, 183, 295
Toomre, A., & Toomre, J. 1972, ApJ, 178, 623
Tremonti, C. A., et al. 2004, ApJ, 613, 898
Tremonti, C. A., Moustakas, J., & Diamond-Stanic, A. M. 2007, ApJ, 663, L77
van den Bergh, S. 2009, ApJ, 702, 1502
van der Wel, A. 2008, ApJ, 675, L13
van der Wel, A., Bell, E. F., Holden, B. P., Skibba, R. A., & Rix, H.-W. 2010, ApJ, 714, 1779
van der Wel, A., et al. 2011, ApJ, 730, 38
van der Wel, A., & van der Marel, R. P. 2008, ApJ, 684, 260
van Dokkum, P. G., et al. 2008, ApJ, 677, L5
Vergani, D., et al. 2010, A&A, 509, A42+
Warren, S. J., et al. 2007, MNRAS, 375, 213
Weinmann, S. M., Kauffmann, G., von der Linden, A., & De Lucia, G. 2010, MNRAS, 406, 2249
Weinmann, S. M., van den Bosch, F. C., & Pasquali, A. 2011, arXiv:1101.3244
Whitaker, K. E., et al. 2010, ApJ, 719, 1715
Williams, R. J., Quadri, R. F., Franx, M., van Dokkum, P., & Labbé, I. 2009, ApJ, 691, 1879
Wuyts, S., et al. 2011a, ApJ, 738, 106
Wuyts, S., et al. 2011b, arXiv:1107.0317
Wuyts, S., et al. 2009, ApJ, 700, 799
Wuyts, S., et al. 2007, ApJ, 655, 51
Wuyts, S., Labbé, I., Schreiber, N. M. F., Franx, M., Rudnick, G., Brammer, G. B., & van Dokkum, P. G. 2008, ApJ, 682, 985
Yi, S. K., et al. 2005, ApJ, 619, L111
Zheng, X. Z., Bell, E. F., Papovich, C., Wolf, C., Meisenheimer, K., Rix, H.-W., Rieke, G. H., & Somerville, R. 2007, ApJ, 661, L41

APPENDIX

APPENDIX A: NORMALIZING THE SAMPLE TO A CONSTANT COMOVING VOLUME

In Fig. 3, we Monte Carlo subsampled the galaxy population of the UDS and the SDSS to an equivalent comoving volume of $10^5\mathrm{Mpc}^3$. There are two ways to do this: simply rescaling the sample by $10^5\mathrm{Mpc}^3/V(z)$, where $V(z)$ is the comoving volume of that redshift bin (leaving one susceptible to the first-order effects of sample variance), or by rescaling the sample in a given redshift bin to have the number of galaxies expected at that redshift above that mass limit using mass functions derived from

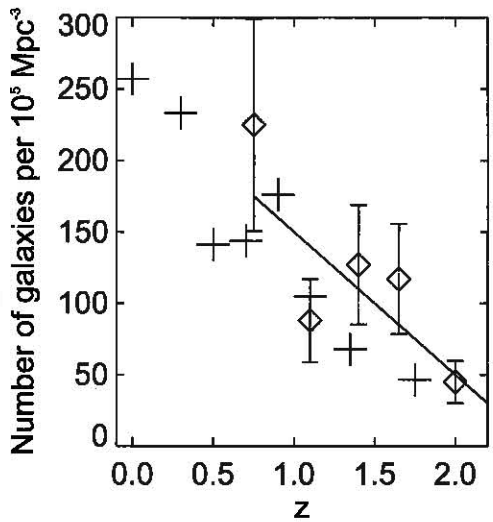

FIG. 11.— The number of galaxies with stellar masses in excess of $3 \times 10^{10} M_\odot$ in a volume of 10^5Mpc^3 measured from the UDS (diamonds, with the dominant sample variance uncertainties as estimated using the method of Somerville et al. 2004; see also Moster et al. 2011), and the number of galaxies with masses in excess of $3 \times 10^{10} M_\odot$ (crosses) inferred from the stellar mass functions of Ilbert et al. (2010, $z > 0.2$) and Bell et al. (2003, local values). The number of galaxies with $M_* > 3 \times 10^{10} M_\odot$ in the UDS is consistent to within the significant sample variance and systematic stellar mass uncertainties with those of larger fields. We choose in this paper to adjust the number of galaxies for display in Fig. 3 to fit the straight line in this figure, to take out the first-order effects of sample variance on the results (while noting that doing so makes no important difference to our conclusions; the evolution of the population is not subtle).

much larger surveys (canceling out number density variation from sample variance, but leaving behind any systematic variation in galaxy properties that are a function of the variation in the average environment in this light cone as a function of redshift).

We compare the two approaches in Fig. 11. Diamonds with error bars denote the number of galaxies with stellar masses in excess of $3 \times 10^{10} M_\odot$ in the UDS, with error bars denoting the expected degree of sample variance in that bin following the method of Somerville et al. (2004). Crosses at $z > 0.2$ show the number of galaxies with stellar mass in excess of $3 \times 10^{10} M_\odot$ expected from the stellar mass functions of Ilbert et al. (2010). The cross at low redshift shows the number of galaxies with $M_* > 3 \times 10^{10} M_\odot$ from the mass function of Bell et al. (2003). The number of galaxies observed in the UDS is broadly consistent with, or perhaps somewhat larger than, the number of galaxies expected from larger surveys, given the substantial sample variance uncertainties. There are systematic uncertainties also on the crosses; choosing different star formation histories for constructing stellar masses, stellar population models, etc., can give more than a factor of two variation in stellar masses that translates into around 50% number density uncertainty. For Fig. 3, we chose to rescale the number of galaxies to the smoothly-varying number of galaxies given by the line shown in Fig. 11 (approximately corresponding to scaling the number of galaxies to larger cosmological surveys).

None of the results shown in Fig. 3 depend in any important way on the choice of this scaling method; the evolution of the galaxy population from $z \sim 2$ to the present day is not subtle and is robust to even the significant systematic uncertainties inherent to mass function analyses. While this scaling in the number of galaxies largely counteracts the worst effects of sample variance, if the properties of galaxies depend strongly on environment there will be a second-order difference between the properties of galaxies sampled from a globally-underdense vs. a globally-overdense volume. In the absence of enough environmental dynamic range to robustly measure its effect within CANDELS at the current time (see Papovich et al. 2011 for a discussion of SFR and galaxy size differences as a function of environment of this using a known $z = 1.62$ galaxy cluster in the CANDELS UDS coverage), we made no attempt to correct for this second-order effect in this paper.